Available online at www.sciencedirect.com
SCIENCE DIRECT
Journal of Sound and Vibration 296 (2006) 690–713
JOURNAL OF SOUND AND VIBRATION
www.elsevier.com/locate/jsvi

Integral equation formulation and analysis of the dynamic stability of damped beams subjected to subtangential follower forces

Z. Elfelsoufi, L. Azrar*

Equipe de Modélisation Mathématique et Contrôle, UFR MAM Faculté des Sciences et Techniques de Tanger, Université Abdelmalek Essaädi, BP. 416, Tanger, Morocco

Received 20 December 2004; received in revised form 1 December 2005; accepted 12 January 2006
Available online 5 July 2006

Abstract

This paper presents a mathematical model based on integral equations for numerical investigations of stability analyses of damped beams subjected to subtangential follower forces. A mathematical formulation based on Euler–Bernoulli beam theory is presented for beams with variable cross sections on a viscoelastic foundation and subjected to lateral excitation, conservative and non-conservative axial loads. Using the boundary element method and radial basis functions, the equation of motion is reduced to an algebro-differential system related to internal and boundary unknowns. Generalized formulations for the deflection, the slope, the moment and the shear force are presented. The free vibration of loaded beams is formulated in a compact matrix form and all necessary matrices are explicitly given. The load–frequency dependence is extensively investigated for various parameters of non-conservative loads, of internal and viscous dampings and for various positions of the concentrated foundation. For an undamped beam, a dynamic stability analysis is illustrated numerically based on the coalescence criterion. The flutter load and instability regions with respect to various parameters are identified. The effects of internal and viscous dampings on the critical flutter load are examined separately and relative effects are evaluated. The dynamic responses, before, near and after the flutter are investigated. A simple and quite general methodological approach is presented. Comprehensive numerical tests for flutter analysis are reported and discussed.

1. Introduction

Flutter instability can occur in a number of engineering structures, such as bridges, pipes, hydrofoils, automotive disks, drum break, rocket and jet engine systems. Although, the origin of the flutter problem lies historically in the aeronautical engineering field, many of its fundamental principles can generally be applied to civil engineering structures. The structural model based on beam theory has often been used to idealize

*Corresponding author. Tel.: +212 39 39 39 54/55; fax: +212 39 39 39 53.
E-mail addresses: azrar@fstt.ac.ma, azrar@hotmail.com (L. Azrar).

0022-460X/$ - see front matter © 2006 Elsevier Ltd. All rights reserved.
doi:10.1016/j.jsv.2006.01.019

many thin structures especially those with long spans. Therefore, vibration and stability problems of beams have long attracted attention in modeling and applied mechanics communities. Using analytical, semi-analytical and numerical methods, the dynamic stability of beams has been investigated in several studies.

For a non-conservative system, a comprehensive discussion of this subject based on analytical procedures can be found in the books [1–3]. Several reviews of problems involving follower forces have been published. A retrospective on the important developments in dynamic stability theory was presented by Bolotin [4]. A comprehensive review with emphasis on canonical problems, i.e.: Beck's, Reut's, Leipholz's and Hauger's columns and experimental work was recently published by Langthjem and Sugiyama [5]. For these problems, it is well known that the usual Euler method and minimum potential energy methods (static methods) are inadequate to predict their instability and that a dynamic method must be employed. The instability analysis of beams under non-conservative forces characterized by flutter which occurs when two of the natural frequencies coincide to become complex conjugate with a positive real part can be done only dynamically. The presence of non-conservative loads makes the system of equations mathematically non-self-adjoint and the corresponding eigenvalue problem is depicted by a non-symmetric matrix. Physically, the instability of the system manifests itself in oscillations with unbounded increasing amplitude when the two lowest eigenvalues become complex conjugates. In recent years, many authors have studied the dynamic stability of elastic structures subjected to subtangential forces, which are a combination of axial and tangential follower forces, and various analytical and numerical procedures have been established for their solutions.

Amongst the numerical methods available for thin structure problems, the finite element method (FEM) is undoubtedly the most versatile. The only problem with this method is that its formulation is quite laborious and it takes a large amount of computer storage. A powerful alternative method based on integral equations is the boundary element method (BEM). The main reason for the rapid development of the BEM is the possibility of reduced dimensionality of the problem, which leads to a reduced set of equations and a smaller amount of data required for the computation. Using the fundamental solution corresponding to the exact solution of a part of the problem, the inappropriate terms are moved to the right-hand side of the governing equation and considered as a fictitious source density. For dynamic instability of beams under elastic foundations and subtangential follower forces, domain integrals are necessary in the formulation. Thus, the main advantage of the dimensionality reduction is eliminated. However, the use of dual reciprocity method (DRM), introduced by Nardini and Brebbia [6], permits the combination of dimensionality reduction advantage with a simple fundamental solution and to formulate the problem on boundary unknowns only. A comprehensive literature review of the DRM and multiple reciprocity method (MRM) as applied to elastodynamics can be found in the review paper of Beskos [7]. Details and applications to various engineering problems are clearly presented in the book of Partridge et al. [8]. Combining the MRM and singular value decomposition method, the rod vibration problem has been analyzed by Chang et al. [9]. Using DRM and the differential quadrature method, the longitudinal vibration of plates and membranes were investigated by Tanaka and Chen [10]. For bending problems of inhomogeneous Euler–Bernoulli beams, an investigation was carried out by Rong et al. [11]. Based on Timoshenko's beam theory and a quadrature method, the dynamic behavior of beams has been analyzed by Schanz and Antes [12]. An extension to beams with arbitrary cross section has been developed by Sapountzakis [13] and to the nonlinear dynamic analysis of beams with variable cross section by Katsikadelis and Tsiatas [14].

There are many other methods used for the flutter phenomenon. The Galerkin and Ritz methods have been used by Levinson [15] for non-conservative problems of elastic structures. The effect of an intermediate support on the dynamic behavior of cantilever beams subjected to follower forces using a discretization method was discussed by Rosa and Franciosi [16]. A variety of subtangential force parameters, various positions, various amplitudes of concentrated or uniform elastic foundations and various boundary conditions were examined. The jump phenomenon was earlier reported by Zorii and Chermokha [17] and in a series of papers by Kounadis [18–20]. Using computerized symbolic algebra in conjunction with the two-term Galerkin method, the same problems have been traited by Elishakoff and Hollkamp [21]. Similarly, the flutter and internal damping effects on the dynamic stability of rods with intermediate spring supports and with relocatable lumped mass under follower loads have been largely investigated by Lee [22–26]. The influence of the subtangential coefficient of follower load and the elastically restrained boundary conditions on the elastic

instability of beams has been discussed by Lee and Hsu [27]. Enhancing flutter and buckling capacity of beams by using piezoelectric layer is presented by Wang and Quek [28]. Based on the FEM, the stability and instability of cantilever elastic beams subjected to a follower force have been investigated by Gasparini et al. [29], Ryu and Sugiyama [30] and Zuo and Schreyer [31]. The divergence and flutter instabilities are generally analyzed by analytical methods or by FEMs.

To the best knowledge of the authors, there is no available compact formulation and results based on the integral equation formulation for buckling, flutter and vibration analyses of thin structures. A formulation based on integral equations and investigations of buckling, vibration and flutter behavior of beams (Beck's problem) have been presented in Refs. [32,33]. A wealth of information has been given in Ref. [33]. This paper intends to extend the previous formulation to damped beams on elastic foundations and subject to various types of follower loads. A simple and general methodological approach is presented. Emphasis is on the effects of the subtangential follower force parameters, the foundation amplitude and position and the damping on the flutter load and limit.

In this paper, a mathematical model based on the integral equations for divergence and flutter instability analyses of damped beams is presented. The Euler–Bernoulli beam theory is used and the governing equation is formulated for beams on a viscoelastic foundation and subject to subtangential follower loads. The radial basis functions and uniform internal discretization are used and all required matrices are explicitly formulated. A generalized formulation for the deflection, the slope, the moment and the shear force are presented and the solution can be obtained at interior or boundary points. The free vibration of loaded beams is formulated in a compact matrix form. The required matrices are explicitly given for numerical investigations. The load–frequency dependence is extensively analyzed for various parameters. The flutter load variations with respect to the position and amplitude of the foundation, the internal and viscous dampings and the flutter zone are investigated. The dynamic response formulation based on modal analysis is established. Numerical results are presented for a clamped–free (C–F) beam submitted to subtangential load and unit impulse at various load levels.

2. Basic beam equations

Let us consider a slender beam of length L with a variable cross section. Using the Euler–Bernoulli beam theory and neglecting the axial displacement, the equation of motion is formulated using the transverse displacement only. The governing partial differential equation of motion of damped beams on a viscoelastic foundation and subjected to axial compression and lateral excitation (Fig. 1) is formulated by

$$\frac{\partial^2}{\partial z^2}\left(EI(z)\left(\frac{\partial^2}{\partial z^2}V(z,t)+\eta\frac{\partial V(z,t)}{\partial t}\right)\right)+\rho(z)S(z)\frac{\partial}{\partial t}\left(\xi V(z,t)+\frac{\partial V(z,t)}{\partial t}\right)$$
$$+\lambda\frac{\partial^2 V(z,t)}{\partial z^2}+\kappa(z)\left(V(z,t)+\upsilon\frac{\partial V(z,t)}{\partial t}\right)=p(z,t), \tag{1}$$

where V is the transverse displacement, E, I, S and ρ are Young's modulus, inertia, the area and the mass density, respectively. $\kappa(z)$ is the elastic foundation, λ is the subtangential load, $p(z,t)$ is the lateral excitation

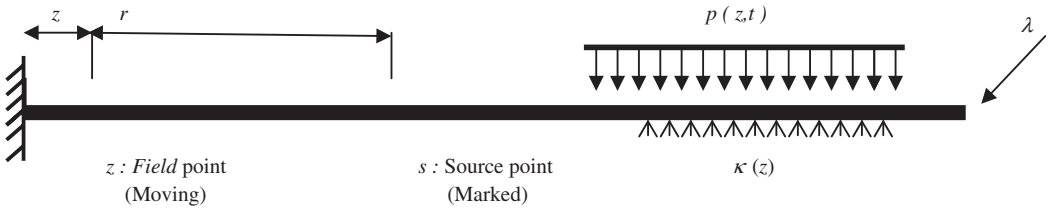

Fig. 1. (C–F) beam subjected to subtangential axial force λ, elastic foundation κ and lateral excitation $p(z,t)$.

and z is the axial coordinate. η, ξ and υ are, respectively, the internal rigidity damping, the internal mass damping and the foundation viscosity factors. For homogeneous beams with a variable cross section, the parameters E, I, S and ρ can be assumed in the following form:

$$EI(z) = E(0)I(0)K_1(z) \quad \text{and} \quad \rho(z)S(z) = \rho(0)S(0)K_2(z), \tag{2}$$

where K_1 and K_2 are functions of the axial coordinate z. Using non-dimensional parameters and Eq. (2), Eq. (1) can be written as

$$\frac{\partial^2}{\partial x^2}\left(K_1(x)\frac{\partial^2}{\partial x^2}(W(x,\tau)+\eta^*\dot{W}(x,\tau))\right)+K_2(x)(\ddot{W}(x,\tau)+\xi^*\dot{W}(x,\tau)) + \lambda^*\frac{\partial^2 W}{\partial x^2}(x,\tau)+\kappa^*(x)(W(x,\tau)+\upsilon^*\dot{W}(x,\tau))=p^*(x,\tau), \tag{3}$$

where

$$\chi=\frac{\rho S(0)L^4}{EI(0)}, \lambda^*=\lambda\frac{L^2}{EI(0)}, \quad \kappa^*=\kappa\frac{L^4}{EI(0)}, \quad \eta^*=\eta\frac{1}{\chi}, \quad \xi^*=\xi\chi, \quad \upsilon^*=\frac{\upsilon}{\chi},$$
$$p^*=p\frac{L^3}{EI(0)}, \quad W(x,\tau)=\frac{V(z,t)}{R}, \quad \tau=\frac{t}{\chi}, \quad R=\sqrt{\frac{I}{S}} \quad \text{and} \quad x=\frac{z}{L}, \tag{4}$$

in which R is the radius of gyration of the beam, $0\leqslant x\leqslant 1$ and the over dot $(\dot{})$ indicates the time derivative.

The aim of this paper is the development of the integral equation formulations for numerical solutions of Eq. (3) and the investigation of the dynamic stability analyses of beams with various parameters of external and internal dampings, elastic foundations and subtangential loads.

3. Integral equation formulation

The fundamental solution of Eq. (3) is difficult to explicitly determine due to the variable coefficients $K_1(x), K_2(x)$ and to the other parameters. As domain integrals are then inevitable, a simple fundamental solution will be used and the resulting domain integrals will be treated by the DRM. Let us denote W^* as the fundamental solution of the following problem:

$$\frac{\partial^2}{\partial x^2}\left(K_1(x)\frac{\partial^2 W^*(x,s)}{\partial x^2}\right)=\delta(x,s), \tag{5}$$

where δ is the Dirac function and 's' is the source point. This fundamental solution will be used and the partial differential equation (3) will be transformed into an integral equation. Following the BEM procedure [6–13,33], the resulting integral equation will be reduced to an algebro-differential equation.

As is well known in the bending problem of beams, the following variables have physical meanings and may be also known at boundaries:

$$\theta(x)=\frac{\partial W}{\partial x}, \quad M(x)=-K_1(x)\frac{\partial^2 W}{\partial x^2} \quad \text{and} \quad Q(x)=\frac{\partial M}{\partial x}, \tag{6}$$

where $\theta(x)$ is the slope, $M(x)$ is the bending moment and $Q(x)$ is the shear force related to the derivatives of the deflection W. These parameters have then to be introduced in the formulation. Multiplying Eq. (3) by W^* and

integrating from 0 to 1, one obtains:

$$\begin{aligned}\int_0^1 \frac{\partial^2}{\partial x^2}\left(K_1(x)\frac{\partial^2}{\partial x^2}(W(x,\tau)+\eta^*\dot{W}(x,\tau))\right)W^*(s,x)\,\mathrm{d}x\\ =-\lambda^*\int_0^1\frac{\partial^2 W}{\partial x^2}(x,\tau)W^*(s,x)\,\mathrm{d}x-\int_0^1 K_2(x)(\ddot{W}(x,\tau)+\xi^*\dot{W}(x,\tau))W^*(s,x)\,\mathrm{d}x\\ -\int_0^1\kappa^*(x)(W(x,\tau)+\upsilon^*\dot{W}(x,\tau))W^*(s,x)\,\mathrm{d}x+\int_0^1 p^*(x,\tau)\,W^*(s,x)\,\mathrm{d}x.\end{aligned}\tag{7}$$

In order to ease the notation, the time variable will be dropped. Integrating by parts four times, the first term of Eq. (7) becomes:

$$\begin{cases}\int_0^1\frac{\partial^2}{\partial x^2}\left(K_1(x)\frac{\partial^2}{\partial x^2}(W(x)+\eta^*\dot{W}(x))\right)W^*(s,x)\,\mathrm{d}x=W(s)+A(s)+\eta^*(\dot{W}(s)+\dot{A}(s)),\\ A(s)=\left[-W^*(s,x)Q(x)+\frac{\partial W^*}{\partial x}(s,x)M(x)+K_1\frac{\partial^2 W^*}{\partial x^2}(s,x)\theta(x)-\frac{\partial}{\partial x}\left(K_1\frac{\partial^2 W^*}{\partial x^2}\right)(s,x)W(x)\right]_0^1,\\ \dot{A}(s)=\left[-W^*(s,x)\dot{Q}(x)+\frac{\partial W^*}{\partial x}(s,x)\dot{M}(x)+K_1\frac{\partial^2 W^*}{\partial x^2}(s,x)\,\dot{\theta}(x)-\frac{\partial}{\partial x}\left(K_1\frac{\partial^2 W^*}{\partial x^2}\right)(s,x)\dot{W}(x)\right]_0^1.\end{cases}\tag{8}$$

On the right-hand side of Eq. (7), three domain integrals have to be evaluated. Making use of radial basis functions, thus avoiding the additional task of domain integration, these domain integrals are transformed into boundary values. To this end, let us assume that for these integrals, the function $W(x,\tau)$ is assumed to be

$$W(x,\tau)=\sum_{j=1}^{n+2}\alpha_j(\tau)f_j(x),\tag{9}$$

where f_j are radial basis functions, 'n' is the number of interior points, α_j are undetermined coefficients [6,8]. Given f_j defines two other functions g_j and h_j which satisfy the following equations:

$$\frac{\mathrm{d}^4 g_j}{\mathrm{d}x^4}(x)=f_j(x)\quad\text{and}\quad\frac{\mathrm{d}^4 h_j}{\mathrm{d}x^4}(x)=K_2(x)f_j(x).\tag{10}$$

More details about W^*, f_j, g_j and h_j, used in this analysis, are given in Appendix A. The mathematical formulation presented here is kept in a general form in order to investigate the dynamic stability analysis of beams with variable cross sections. Making use of these transformations, it is now possible to evaluate the integral formulation (7) using boundary values only. Based on the decomposition (9) and Eq. (10), the three domain integrals on the r.h.s. of Eq. (7) are transformed into boundary values as follows:

$$\begin{cases}-\int_0^1 K_2(x)(\ddot{W}(x)+\xi^*\dot{W}(x))W^*(s,x)\,\mathrm{d}x=-\sum_{j=1}^{n+2}[(\ddot{\alpha}_j B_j(s)+\xi^*\dot{\alpha}_j B_j(s)],\\ B_j(s)=h_j(s)+\left[W^*(s,x)\frac{\mathrm{d}^3 h_j}{\mathrm{d}x^3}(x)-\frac{\partial W^*}{\partial x}(s,x)\frac{\mathrm{d}^2 h_j}{\mathrm{d}x^2}(x)+\frac{\partial^2 W^*}{\partial x^2}(s,x)\frac{\mathrm{d}h_j}{\mathrm{d}x}(x)-\frac{\partial^3 W^*}{\partial x^3}(s,x)h_j(x)\right]_0^1,\end{cases}\tag{11a}$$

$$\begin{cases}-\lambda^*\int_0^1\left(\frac{\partial^2 W}{\partial x^2}(x)\right)W^*(s,x)\,\mathrm{d}x=-\lambda^*\sum_{j=1}^{n+2}\alpha_j C_j(s),\\ C_j(s)=\frac{\mathrm{d}^2 g_j}{\mathrm{d}x^2}(s)+\left[W^*(s,x)\frac{\mathrm{d}^5 g_j}{\mathrm{d}x^5}(x)-\frac{\partial W^*}{\partial x}(s,x)\frac{\mathrm{d}^4 g_j}{\mathrm{d}x^4}(x)+\frac{\partial^2 W^*}{\partial x^2}(s,x)\frac{\mathrm{d}^3 g_j}{\mathrm{d}x^3}(x)\right.\\ \qquad\left.-\frac{\partial^3 W^*}{\partial x^3}(s,x)\frac{\mathrm{d}^2 g_j}{\mathrm{d}x^2}(x)\right]_0^1.\end{cases}\tag{11b}$$

For a uniform elastic foundation:

$$\begin{cases} -\int_0^1 \kappa^*(x)(W(x)+\upsilon^*\dot{W}(x))W^*(s,x)\,\mathrm{d}x = -\kappa^*\sum_{j=1}^{n+2}(\alpha_j+\upsilon^*\dot{\alpha}_j)D_j(s), \\ D_j(s) = g_j(s) + \left[W^*(s,x)\dfrac{\mathrm{d}^3 g_j}{\mathrm{d}x^3}(x) - \dfrac{\partial W^*}{\partial x}(s,x)\dfrac{\mathrm{d}^2 g_j}{\mathrm{d}x^2}(x)\right. \\ \qquad \left. + \dfrac{\partial^2 W^*}{\partial x^2}(s,x)\dfrac{\mathrm{d}g_j}{\mathrm{d}x}(x) - \dfrac{\partial^3 W^*}{\partial x^3}(s,x)g_j(x)\right]_0^1. \end{cases} \tag{11c}$$

For a concentrated elastic foundation κ^* at the point x_c:

$$\begin{cases} -\int_0^1 \kappa^*(x)\big(W(x)+\upsilon^*\dot{W}(x)\big)W^*(s,x)\,\mathrm{d}x = -\kappa^*\sum_{j=1}^{n+2}(\alpha_j+\upsilon^*\dot{\alpha}_j)D_j(s), \\ D_j(s) = 0 \text{ for } j\neq c \quad \text{and } D_c(s) = W(x_c)\,W^*(s,x_c) \end{cases} \tag{11d}$$

Let us recall that the damping coefficient υ^* is associated to the viscous foundation κ^* and if the foundation is concentrated the viscous damping is concentrated too. The transverse excitation load is given by

$$P(s,t) = \int_0^1 p^*(x,t)W^*(s,x)\,\mathrm{d}x. \tag{11e}$$

Based on the later transformations, the integral equation formulation (7) is reduced to the following algebro-differential equation at interior points:

$$\begin{aligned} W(s)+A(s)+\eta^*(\dot{W}(s)+\dot{A}(s)) = & -\sum_{j=1}^{n+2}(\ddot{\alpha}_j B_j(s)+\xi^*\dot{\alpha}_j B_j(s)) \\ & -\lambda^*\sum_{j=1}^{n+2}\alpha_j C_j(s) - \kappa^*\sum_{j=1}^{n+2}(\alpha_j D_j(s)+\upsilon^*\dot{\alpha}_j D_j(s)) + P(s), \end{aligned} \tag{12}$$

or

$$\begin{aligned} W(s)+A(s)+\eta^*(\dot{W}(s)+\dot{A}(s)) = & -\sum_{j=1}^{n+2}\ddot{\alpha}_j B_j(s) - \sum_{j=1}^{n+2}\alpha_j(\lambda^* C_j(s)+\kappa^* D_j(s)) \\ & -\sum_{j=1}^{n+2}\dot{\alpha}_j(\xi^* B_j(s)+\kappa^*\upsilon^* D_j(s)) + P(s). \end{aligned} \tag{13}$$

In order to present a well-posed problem in its general formulation, more equations than Eq. (13) related to θ, M and Q are required. They are obtained by derivatives of Eq. (13) with respect to the variable s. For a compact equation representation, the following notations are introduced:

$$\hat{E}(s) = \frac{\partial E}{\partial s}(s), \quad \hat{\hat{E}}(s) = K_1(s)\frac{\partial \hat{E}}{\partial s}(s) \quad \text{and} \quad \hat{\hat{\hat{E}}}(s) = \frac{\partial \hat{\hat{E}}}{\partial s}(s), \tag{14}$$

where E may be: A, B, C or $E = D$.

Finally, one obtains for a uniform elastic foundation the following algebro-differential system:

$$\begin{cases} [W(s)+A(s)]+\eta^*[\dot{W}(s)+\dot{A}(s)] = -\sum_{j=1}^{n+2}\{\ddot{\alpha}_j B_j(s)+\alpha_j(\lambda^* C_j(s)+\kappa^* D_j(s))\} \\ \qquad\qquad -\sum_{j=1}^{n+2}\dot{\alpha}_j\{\xi^* B_j(s)+\kappa^*\upsilon^* D_j(s)\}+P(s), \\ [\theta(s)+\hat{A}(s)]+\eta^*[\dot{\theta}(s)+\dot{\hat{A}}(s)] = -\sum_{j=1}^{n+2}\{\ddot{\alpha}_j \hat{B}_j(s)+\alpha_j(\lambda^* \hat{C}_j(s)+\kappa^* \hat{D}_j(s))\} \\ \qquad\qquad -\sum_{j=1}^{n+2}\dot{\alpha}_j\{\xi^* \hat{B}_j(s)+\kappa^*\upsilon^* \hat{D}_j(s)\}+\hat{P}(s), \\ [-M(s)+\hat{\hat{A}}(s)]+\eta^*[-\dot{M}(s)+\dot{\hat{\hat{A}}}(s)] = -\sum_{j=1}^{n+2}\{\ddot{\alpha}_j \hat{\hat{B}}_j(s)+\alpha_j(\lambda^* \hat{\hat{C}}_j(s)+\kappa^* \hat{\hat{D}}_j(s))\} \\ \qquad\qquad -\sum_{j=1}^{n+2}\dot{\alpha}_j\{\xi^* \hat{\hat{B}}_j(s)+\kappa^*\upsilon^* \hat{\hat{D}}_j(s)\}+\hat{\hat{P}}(s), \\ [-Q(s)+\hat{\hat{\hat{A}}}(s)]+\eta^*[-\dot{Q}(s)+\dot{\hat{\hat{\hat{A}}}}(s)] = -\sum_{j=1}^{n+2}\{\ddot{\alpha}_j \hat{\hat{\hat{B}}}_j(s)+\alpha_j(\lambda^* \hat{\hat{\hat{C}}}_j(s)+\kappa^* \hat{\hat{\hat{D}}}_j(s))\} \\ \qquad\qquad -\sum_{j=1}^{n+2}\dot{\alpha}_j\{\xi^* \hat{\hat{\hat{B}}}_j(s)+\kappa^*\upsilon^* \hat{\hat{\hat{D}}}_j(s)\}+\hat{\hat{\hat{P}}}(s). \end{cases} \tag{15}$$

These equations give analytical solution representations with respect to the interior variable 's' for the transverse displacement, slope, moment and shear force. For a numerical solution, a discretization of Eq. (15) and the consideration of boundary conditions are needed.

4. Matrix formulations

After discretization of Eq. (15), one can write:

$$W_i + A_i + \eta^*(\dot{W}_i + \dot{A}_i) = -\sum_{j=1}^{n+2}\{\ddot{\alpha}_j B_{ij} + \dot{\alpha}_j(\xi^* B_{ij} + \kappa^*\upsilon^* D_{ij}) + \alpha_j(\lambda^* C_{ij} + \kappa^* D_{ij})\} + P_i, \tag{16a}$$

$$\theta_i + \hat{A}_i + \eta^*(\dot{\theta}_i + \dot{\hat{A}}_i) = -\sum_{j=1}^{n+2}\{\ddot{\alpha}_j \hat{B}_{ij} + \dot{\alpha}_j(\xi^* \hat{B}_{ij} + \kappa^*\upsilon^* \hat{D}_{ij}) + \alpha_j(\lambda^* \hat{C}_{ij} + \kappa^* \hat{D}_{ij})\} + \hat{P}_i, \tag{16b}$$

$$-M_i + \hat{\hat{A}}_i + \eta^*(-\dot{M}_i + \dot{\hat{\hat{A}}}_i) = -\sum_{j=1}^{n+2}\{\ddot{\alpha}_j \hat{\hat{B}}_{ij} + \dot{\alpha}_j(\xi^* \hat{\hat{B}}_{ij} + \kappa^*\upsilon^* \hat{\hat{D}}_{ij}) + \alpha_j(\lambda^* \hat{\hat{C}}_{ij} + \kappa^* \hat{\hat{D}}_{ij})\} + \hat{\hat{P}}_i, \tag{16c}$$

$$-Q_i + \hat{\hat{\hat{A}}}_i + \eta^*(-\dot{Q}_i + \dot{\hat{\hat{\hat{A}}}}_i) = -\sum_{j=1}^{n+2}\{\ddot{\alpha}_j \hat{\hat{\hat{B}}}_{ij} + \dot{\alpha}_j(\xi^* \hat{\hat{\hat{B}}}_{ij} + \kappa^*\upsilon^* \hat{\hat{\hat{D}}}_{ij}) + \alpha_j(\lambda^* \hat{\hat{\hat{C}}}_{ij} + \kappa^* \hat{\hat{\hat{D}}}_{ij})\} + \hat{\hat{\hat{P}}}_i \tag{16d}$$

in which $i = 1$ and $n+2$ correspond to the beam ends and $i = 2$ to $n+1$ correspond to interior points which may correspond to a uniform or a non-uniform discretization (Fig. 2).

Let us recall that we have $(n+4)$ unknowns, (n) interior W_i and four unknowns related to the assumed boundary conditions. Eq. (16a) leads to $(n+2)$ equations and two extra equations are then needed. Eqs. (16b)

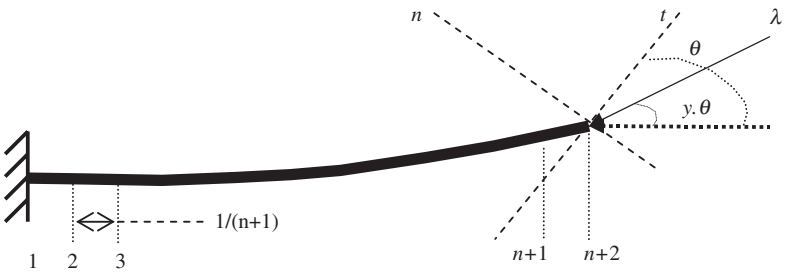

Fig. 2. Uniform discretization of a clamped–free beam and load parameters ($W_1 = 0$, $\theta_1 = 0$, $M_{n+2} = 0$ and $Q_{n+2} = -\kappa^* W_{n+2} + (1-y)\lambda\theta_{n+2}$).

or (16c) may be used to complete the system for a (C–F) boundary condition. A combination of Eqs. (16a)–(16d) can also be used to solve the system for more general boundary conditions. Based on the coordinate functions given in Ref. [8], for the static case, the unknown function vector $\{\alpha\}$ and its time derivatives can be written in the following form:

$$\boldsymbol{\alpha} = \mathbf{G}\mathbf{W}, \quad \dot{\boldsymbol{\alpha}} = \mathbf{G}\dot{\mathbf{W}} \quad \text{and} \quad \ddot{\boldsymbol{\alpha}} = \mathbf{G}\ddot{\mathbf{W}}, \tag{17}$$

where $\mathbf{G}$ is the radial basis function matrix and it is explicitly given in Appendix B. For a (C–F) beam subjected to a subtangential follower force, as presented in Fig. 2, the boundary conditions are expressed as: $W_1 = 0$, $\theta_1 = 0$, $M_{n+2} = 0$ and $Q_{n+2} = -\kappa^*(W_{n+2} + \upsilon^* \dot{W}_{n+2}) + (1-y)\lambda^*\theta_{n+2}$. The parameter '$y$' is used to denote the combination such that '$y = 0$' describes the axial load and '$y \neq 0$' the follower force. Only '$y = 0$' provides a conservative loading. The term $\lambda^*(1-y)\theta_{n+2}$ is moved to the right-hand side. The unknowns at boundary and interior points are expressed by the following vector notations:

$$\mathbf{W} = \{W_2, W_3, \ldots, W_{n+1}, W_{n+2}, \theta_{n+2}\} \quad \text{and} \quad \mathbf{T} = \{M_1, Q_1\}, \tag{18a}$$

$$\dot{\mathbf{W}} = \{\dot{W}_2, \dot{W}_3, \ldots, \dot{W}_{n+1}, \dot{W}_{n+2}, \dot{\theta}_{n+2}\} \quad \text{and} \quad \dot{\mathbf{T}} = \{\dot{M}_1, \dot{Q}_1\}. \tag{18b}$$

As W_1, θ_1 and M_{n+2} are null, they will be eliminated and Eqs. (16a) and (16b) will be used for unknowns. Making use of the considered boundary conditions, the function $A(s)$ in Eq. (8) is rewritten as

$$\begin{aligned} A(s) = {} & \left(\kappa^* W^*(s,1) - \frac{\partial^3 W^*}{\partial x^3}(s,1)\right) W_{n+2} - \left(\lambda^*(1-y)W^*(s,1) - \frac{\partial^2 W^*}{\partial x^2}(s,1)\right)\theta_{n+2} \\ & - \frac{\partial W^*}{\partial x}(s,0)M_1 + W^*(s,0)Q_1 + (\kappa^*\upsilon^* W^*(s,1))\dot{W}_{n+2}. \end{aligned} \tag{19a}$$

In this study, a simple fundamental solution is used, i.e.: $W^*(x,s) = |x-s|^3/12$ (Appendix A). The explicit formulation of $A(s)$ is then given by

$$\begin{aligned} A(s) = {} & \left(\kappa^* \frac{(1-s)^3}{12} - \frac{1}{2}\right) W_{n+2} - \left(\lambda^*(1-y)\frac{(1-s)^3}{12} - \frac{(1-s)}{2}\right)\theta_{n+2} - \frac{s^2}{4}M_1 + \frac{s^3}{12}Q_1 \\ & + \kappa^*\upsilon^* \frac{(1-s)^3}{12}\dot{W}_{n+2}. \end{aligned} \tag{19b}$$

For the sake of clarity, the required equations are explicitly expressed at all unknowns. For the considered boundary conditions '$n+2$' equations are obtained by using Eq. (16a) for $i = 1$ to $n+2$ and two additional

ones are obtained from Eq. (16b) for $i=1$ and $n+2$ as follows:

$$
\begin{cases}
(a)\left[W_2+\left(\kappa^*\dfrac{(1-s_2)^3}{12}-\dfrac{1}{2}\right)W_{n+2}+\dfrac{(1-s_2)}{2}\theta_{n+2}\right]+\left[-\dfrac{s_2^2}{4}M_1+\dfrac{s_2^3}{12}Q_1\right]\\
\quad+\eta^*\left[\dot{W}_2+\left(\kappa^*\dfrac{(1-s_2)^3}{12}-\dfrac{1}{2}\right)\dot{W}_{n+2}+\dfrac{(1-s_2)}{2}\dot{\theta}_{n+2}\right]+\eta^*\left[-\dfrac{s_2^2}{4}\dot{M}_1+\dfrac{s_2^3}{12}\dot{Q}_1\right]=-\left[\sum_{j=1}^{n+2}B_{2j}\,\ddot{W}_j\right]\\
\quad-\kappa^*\eta^*\upsilon^*\left[\dfrac{(1-s_2)^3}{12}\ddot{W}_{n+2}\right]-\lambda^*\left[\sum_{j=1}^{n+2}C_{2j}W_j\right]+\lambda^*(1-y)\left[\dfrac{(1-s_2)^3}{12}\theta_{n+2}\right]-\kappa^*\left[\sum_{j=1}^{n+2}D_{2j}W_j\right]\\
\quad-\left[\sum_{j=1}^{n+2}\{(\xi^*B_{2j}+\kappa^*\upsilon^*D_{2j})\dot{W}_j\}\right]+\eta^*\lambda^*(1-y)\left[\dfrac{(1-s_2)^3}{12}\dot{\theta}_{n+2}\right]-\kappa^*\upsilon^*\left[\dfrac{(1-s_2)^3}{12}\dot{W}_{n+2}\right]+P_2\quad i=2\\
\vdots\qquad\qquad\vdots\qquad\qquad\vdots\qquad\qquad\vdots\\
(b)\ \underbrace{\left[W_i+\left(\kappa^*\dfrac{(1-s_i)^3}{12}-\dfrac{1}{2}\right)W_{n+2}+\dfrac{(1-s_i)}{2}\theta_{n+2}\right]}_{\mathbf{IW}}+\underbrace{\left[-\dfrac{s_i^2}{4}M_1+\dfrac{s_i^3}{12}Q_1\right]}_{\mathbf{AT}}\\
\quad\underbrace{+\eta^*\left[\dot{W}_i+\left(\kappa^*\dfrac{(1-s_i)^3}{12}-\dfrac{1}{2}\right)\dot{W}_{n+2}+\dfrac{(1-s_i)}{2}\dot{\theta}_{n+2}\right]}_{\eta^*\mathbf{I}\dot{\mathbf{W}}}\underbrace{+\eta^*\left[-\dfrac{s_i^2}{4}\dot{M}_1+\dfrac{s_i^3}{12}\dot{Q}_1\right]}_{\eta^*\mathbf{A}\dot{\mathbf{T}}}\\
=\underbrace{-\left[\sum_{j=1}^{n+2}B_{ij}\ddot{W}_j\right]}_{\mathbf{B}\ddot{\mathbf{W}}}\underbrace{-\kappa^*\eta^*\upsilon^*\left[\dfrac{(1-s_i)^3}{12}\ddot{W}_{n+2}\right]}_{\kappa^*\eta^*\upsilon^*\mathbf{H}\ddot{\mathbf{W}}}\underbrace{-\lambda^*\left[\sum_{j=1}^{n+2}C_{ij}W_j\right]}_{\lambda^*\mathbf{BW}}\\
\quad\underbrace{+\lambda^*(1-y)\left[\dfrac{(1-s_i)^3}{12}\theta_{n+2}\right]}_{\lambda^*(1-y)\mathbf{JW}}\\
\quad\underbrace{-\kappa^*\left[\sum_{j=1}^{n+2}D_{ij}W_j\right]}_{\kappa^*\mathbf{DW}}\underbrace{-\left[\sum_{j=1}^{n+2}(\xi^*B_{ij}+\kappa^*\upsilon^*D_{ij})\dot{W}_j\right]}_{(\xi^*\mathbf{B}+\kappa^*\upsilon^*\mathbf{D})\dot{\mathbf{W}}}\underbrace{+\eta^*\lambda^*(1-y)\left[\dfrac{(1-s_i)^3}{12}\dot{\theta}_{n+2}\right]}_{\eta^*\lambda^*(1-y)\mathbf{J}\dot{\mathbf{W}}}\\
\quad\underbrace{-\kappa^*\upsilon^*\left[\dfrac{(1-s_i)^3}{12}\dot{W}\right]}_{k^*\upsilon^*\mathbf{H}\dot{\mathbf{W}}}\underbrace{+P_i}_{\mathbf{P}}\quad i=i\\
\vdots\qquad\qquad\vdots\qquad\qquad\vdots\qquad\qquad\vdots\\
(c)\ \cdots\qquad\qquad\cdots\qquad\qquad\cdots\qquad\qquad\cdots\quad i=n+2\\
(d)\ \left[\left(\dfrac{\kappa^*}{12}-\dfrac{1}{2}\right)W_{n+2}+\dfrac{1}{2}\theta_{n+2}\right]+\eta^*\left[\left(\dfrac{\kappa^*}{12}-\dfrac{1}{2}\right)\dot{W}_{n+2}+\dfrac{1}{2}\dot{\theta}_{n+2}\right]=-\left[\sum_{j=1}^{n+2}B_{1j}\ddot{W}_j\right]\\
\quad-\kappa^*\eta^*\upsilon^*\left[\dfrac{1}{12}\ddot{W}_{n+2}\right]-\lambda^*\left[\sum_{j=1}^{n+2}C_{1j}W_j\right]+\lambda^*(1-y)\left[\dfrac{1}{12}\theta_{n+2}\right]-\kappa^*\left[\sum_{j=1}^{n+2}D_{1j}W_j\right]\\
\quad-\left[\sum_{j=1}^{n+2}\{(\xi^*B_{1,j}+\kappa^*\upsilon^*D_{1j})\dot{W}_j\}\right]+\eta^*\lambda^*(1-y)\left[\dfrac{1}{12}\dot{\theta}_{n+2}\right]-\kappa^*\upsilon^*\left[\dfrac{1}{12}\dot{W}\right]+P_1\quad i=1
\end{cases}
\tag{20}
$$

$$
\begin{cases}
\text{(e)} \left[\dfrac{-\kappa^*}{4} W_{n+2} - \dfrac{1}{2}\theta_{n+2}\right] - \eta^* \left[\dfrac{\kappa^*}{4} \dot{W}_{n+2} + \dfrac{1}{2}\dot{\theta}_{n+2}\right] \\
\quad = -\left[\sum_{j=1}^{n+2} \hat{B}_{1j} \ddot{W}_j\right] - \lambda^* \left[\sum_{j=1}^{n+2} \hat{C}_{1j} W_j\right] - \lambda^*(1-y)\left[\dfrac{1}{4}\theta_{n+2}\right] \\
\quad\quad -\kappa^* \left[\sum_{j=1}^{n+2} \hat{D}_{1j} W_j\right] - \left[\sum_{j=1}^{n+2} \{(\xi^* \hat{B}_{1j} + \kappa^* \upsilon^* \hat{D}_{1j}) \dot{W}_j\}\right] \\
\quad\quad \underbrace{+\kappa^* \eta^* \upsilon^* \left[\dfrac{1}{4} \ddot{W}_{n+2}\right]}_{\kappa^* \eta^* \upsilon^* \mathbf{H}' \ddot{\mathbf{W}}} \underbrace{-\eta^* \lambda^* (1-y)\left[\dfrac{1}{4}\dot{\theta}_{n+2}\right]}_{\eta^* \lambda^* (1-y) \mathbf{J}' \dot{\mathbf{W}}} \underbrace{+\kappa^* \upsilon^* \left[\dfrac{1}{4} \dot{W}_{n+2}\right]}_{\kappa^* \upsilon^* \mathbf{H}' \dot{\mathbf{W}}} + \hat{P}_1 \quad i = 1 \\
\text{(f)} \underbrace{\left[\dfrac{1}{2}\theta_{n+2}\right]}_{\mathbf{O}\dot{\mathbf{W}}} \underbrace{+\left[-\dfrac{1}{2} M_1 + \dfrac{1}{4} Q_1\right]}_{\mathbf{A}\mathbf{T}} \underbrace{+\eta^* \left[\dfrac{1}{2}\dot{\theta}_{n+2}\right]}_{\eta^* \mathbf{O} \dot{\mathbf{W}}} \underbrace{+\dot{\eta}\left[-\dfrac{1}{2}\dot{M}_1 + \dfrac{1}{4}\dot{Q}_1\right]}_{\eta^* \mathbf{A}' \dot{\mathbf{T}}} \\
\quad = \underbrace{-\left[\sum_{j=1}^{n+2} \hat{B}_{n+2,j} \ddot{W}_j\right]}_{\mathbf{B}' \ddot{\mathbf{W}}} \underbrace{-\lambda^* \left[\sum_{j=1}^{n+2} \hat{C}_{n+2,j} W_j\right]}_{\lambda^* \mathbf{C}' \mathbf{W}} \underbrace{-\kappa^* \left[\sum_{j=1}^{n+2} \hat{D}_{n+2,j} W_j\right]}_{\kappa^* \mathbf{D}' \mathbf{W}} \\
\quad\quad \underbrace{-\left[\sum_{j=1}^{n+2} \{(\xi^* \hat{\beta}_{n+2,j} + \kappa^* \upsilon^* \hat{D}_{n+2,j}) \dot{W}_j\}\right]}_{(\xi^* \mathbf{B}' + \kappa^* \upsilon^* \mathbf{D}') \dot{\mathbf{W}}} \underbrace{+\hat{P}_{n+2}}_{\mathbf{P}'} \quad i = n+2
\end{cases}
$$

In which $s_i = (i-1)/(n+1)$. For a compact form, the following matrix formulation is used:

$$
\begin{bmatrix} \mathbf{I}\mathbf{A}\eta^* \mathbf{I}\eta^* \mathbf{A} \\ \mathbf{O}\mathbf{A}'\eta^* \mathbf{O}\eta^* \mathbf{A}' \end{bmatrix} \begin{Bmatrix} \mathbf{W} \\ \mathbf{T} \\ \dot{\mathbf{W}} \\ \dot{\mathbf{T}} \end{Bmatrix} + \left(\begin{bmatrix} \mathbf{B} \\ \mathbf{B}' \end{bmatrix} + \kappa^* \eta^* \upsilon^* \begin{bmatrix} \mathbf{H} \\ \mathbf{H}' \end{bmatrix} \right) \ddot{\mathbf{W}} + \lambda^* \left(\begin{bmatrix} \mathbf{C} \\ \mathbf{C}' \end{bmatrix} + (1-y) \begin{bmatrix} \mathbf{J} \\ \mathbf{J}' \end{bmatrix} \right) \mathbf{W}
$$

$$
+ \kappa^* \begin{bmatrix} \mathbf{D} \\ \mathbf{D}' \end{bmatrix} \mathbf{W} + \left(\xi^* \begin{bmatrix} \mathbf{B} \\ \mathbf{B}' \end{bmatrix} + \kappa^* \upsilon^* \begin{bmatrix} \mathbf{H} \\ \mathbf{H}' \end{bmatrix} + \lambda^* \eta^* (1-y) \begin{bmatrix} \mathbf{J} \\ \mathbf{J}' \end{bmatrix} + \kappa^* \upsilon^* \begin{bmatrix} \mathbf{D} \\ \mathbf{D}' \end{bmatrix} \right) \dot{\mathbf{W}} = \begin{Bmatrix} \mathbf{P} \\ \mathbf{P}' \end{Bmatrix}. \tag{21}
$$

Details about related matrices of Eqs. (21) are given in Appendix B. Eq. (21) presents a differential system with respect to time on the deflection at unknown interior points **W** and unknowns at boundaries represented by **T**. This system is rewritten as:

$$
\begin{cases}
\mathbf{A}'(\mathbf{T} + \eta^* \dot{\mathbf{T}}) + (\mathbf{B}' + \kappa^* \eta^* \upsilon^* \mathbf{H}') \ddot{\mathbf{W}} + (\lambda^* (\mathbf{C}' - (1-y)\mathbf{J}') + \kappa^* \mathbf{D}' - \mathbf{O}) \mathbf{W} \\
\quad + (\xi^* \mathbf{B}' + \kappa^* \upsilon^* \mathbf{H}' + \lambda^* \eta^* (1-y) \mathbf{J}' + \kappa^* \upsilon^* \mathbf{D}' - \eta^* \mathbf{O}) \dot{\mathbf{W}} = \mathbf{P}', \\
\mathbf{A}(\mathbf{T} + \eta^* \dot{\mathbf{T}}) + (\mathbf{B} + \kappa^* \eta^* \upsilon^* \mathbf{H}) \ddot{\mathbf{W}} + (\lambda^* (\mathbf{C} - (1-y)\mathbf{J}) + \kappa^* \mathbf{D} - \mathbf{I}) \mathbf{W} \\
\quad + (\xi^* \mathbf{B} + \kappa^* \upsilon^* \mathbf{H} + \lambda^* \eta^* (1-y) \mathbf{J} + \kappa^* \upsilon^* \mathbf{D} - \eta^* \mathbf{I}) \dot{\mathbf{W}} = \mathbf{P}.
\end{cases} \tag{22a,b}
$$

Eq. (22) permits one to compute the unknowns at boundaries as a function of the interior points by the following equation:

$$
\begin{aligned}
\eta^* \dot{\mathbf{T}} + \mathbf{T} = & -\mathbf{A}'^{-1} [(\xi^* \mathbf{B}' + \kappa^* \upsilon^* \mathbf{H}' + \lambda^* \eta^* (1-y) \mathbf{J}' + \kappa^* \upsilon^* \mathbf{D}' - \eta^* \mathbf{O}) \dot{\mathbf{W}} \\
& + (\mathbf{B}' + \kappa^* \eta^* \upsilon^* \mathbf{H}') \ddot{\mathbf{W}} + (\lambda^* (\mathbf{C}' - (1-y)\mathbf{J}') + \kappa^* \mathbf{D}' - \mathbf{O}) \mathbf{W} - \mathbf{P}'].
\end{aligned} \tag{23a}
$$

The stationary limit condition ($\dot{\mathbf{T}} = \mathbf{0}$) gives

$$\begin{aligned}\mathbf{T} = & -\mathbf{A}'^{-1}[(\xi^*\mathbf{B}' + \kappa^*\upsilon^*\mathbf{H}' + \lambda^*\eta^*(1-y)\mathbf{J}' + \kappa^*\upsilon^*\mathbf{D}' - \eta^*\mathbf{O})\dot{\mathbf{W}} \\ & + (\mathbf{B}' + \kappa^*\eta^*\upsilon^*\mathbf{H}')\ddot{\mathbf{W}} + (\lambda^*(\mathbf{C}' - (1-y)\mathbf{J}') + \kappa^*\mathbf{D}' - \mathbf{O})\mathbf{W} - \mathbf{P}'].\end{aligned} \tag{23b}$$

Using Eq. (23b) and after some mathematical manipulations, Eq. (22) can be transformed into the deflection problem as follows:

$$\mathbf{M}\ddot{\mathbf{W}} + \mathbf{Cd}\dot{\mathbf{W}} + \mathbf{K}\mathbf{W} + \mathbf{f} = \mathbf{0}, \tag{24}$$

where

$$\mathbf{M} = (\mathbf{B} - \mathbf{A}\mathbf{A}'\mathbf{B}') + \kappa^*\eta^*\upsilon^*(\mathbf{H} - \mathbf{A}\mathbf{A}'^{-1}\mathbf{H}'),$$

$$\begin{aligned}\mathbf{Cd} = & \eta^*(\mathbf{A}\mathbf{A}'^{-1}\mathbf{O} - \mathbf{I}) + \xi^*(\mathbf{B} - \mathbf{A}\mathbf{A}'\mathbf{B}') + \kappa^*\upsilon^*(\mathbf{H} - \mathbf{A}\mathbf{A}'^{-1}\mathbf{H}') \\ & + \eta^*(1-y)\mathbf{J} - \mathbf{A}\mathbf{A}'^{-1}\mathbf{J}' + \kappa^*\upsilon^*(\mathbf{D} - \mathbf{A}\mathbf{A}'^{-1}\mathbf{D}'),\end{aligned}$$

$$\boldsymbol{K} = \mathbf{A}\mathbf{A}'^{-1}\mathbf{O} - \mathbf{I} + \kappa^*(\mathbf{D} - \mathbf{A}\mathbf{A}'^{-1}\mathbf{D}') + \lambda^*(\mathbf{C} - \mathbf{A}\mathbf{A}'^{-1}\mathbf{C}' - \mathbf{J} + \mathbf{A}\mathbf{A}'^{-1}\mathbf{J}'),$$

$$\mathbf{f} = \mathbf{P} - \mathbf{A}\mathbf{A}'^{-1}\mathbf{P}'.$$

All the related matrices can be easily computed and explicit expressions are given in Appendix B. It is clearly shown that the matrix **Cd** is damping parameters dependent and the matrix **K** is load and foundation stiffness dependent. These parameters will be chosen and the corresponding dynamic behavior of the beam will be investigated based on Eq. (24).

5. Eigenvalue procedure and decomposition method

The solution of the considered problem will be obtained by numerically solving Eq. (24). By using standard algorithms such as Runge–Kutta or Newmark, the time response may be investigated at interior and boundary points. The deflection time evolution may be then computed with respect to various parameters. The formulation (24) is quite general and it may be used both for dynamic stability and for control analysis. In this paper, we limit ourselves to the eigenvalue procedure and to the decomposition method for dynamic stability analysis.

5.1. Free vibration of loaded beams

Let us assume that the displacement field can be written in the following form:

$$\begin{cases} W(x,\tau) = W(x)\mathrm{e}^{\Omega\tau}, \\ \Omega = \sigma + \mathrm{i}\omega. \end{cases} \tag{25}$$

Neglecting the excitation vector ($\mathbf{f} = \mathbf{0}$) and inserting Eq. (25) into Eq. (24), the following standard eigenvalue problem is obtained:

$$(\Omega^2\mathbf{M} + \Omega\mathbf{Cd} + \mathbf{K})\mathbf{W} = \mathbf{0}. \tag{26a}$$

This equation is recast as a classical eigenvalue problem by

$$\begin{cases} \boldsymbol{\Gamma}\mathbf{Z} = \Omega\mathbf{Z}, \\ \boldsymbol{\Gamma} = \begin{pmatrix} \mathbf{K} & \mathbf{0} \\ \mathbf{0} & \mathbf{M} \end{pmatrix}^{-1} \begin{pmatrix} \mathbf{0} & \mathbf{K} \\ -\mathbf{K} & -\mathbf{C} \end{pmatrix}, \quad \mathbf{Z} = \begin{Bmatrix} \mathbf{W} \\ \Omega\mathbf{W} \end{Bmatrix}. \end{cases} \tag{26b}$$

Remember that the matrix $\mathbf{K}$ is load dependent. The load–frequency analysis is then investigated by numerically solving the eigenvalue problem (26b) for each considered load increment.

5.2. Dynamic response

The dynamic response is obtained by numerically solving the following differential problem:

$$\begin{cases} \dot{\mathbf{Z}} = \mathbf{\Gamma Z} + \mathbf{F}, \\ \mathbf{Z} = \begin{Bmatrix} \mathbf{W} \\ \dot{\mathbf{W}} \end{Bmatrix}; \ \mathbf{F} = \begin{pmatrix} \mathbf{K} & \mathbf{0} \\ \mathbf{0} & \mathbf{M} \end{pmatrix}^{-1} \begin{Bmatrix} \mathbf{0} \\ -\mathbf{f} \end{Bmatrix}. \end{cases} \tag{27}$$

The complete solution is obtained by the following well-known convolution integral involving the transition matrix $\mathbf{exp(\Gamma t)}$:

$$\mathbf{Z(t)} = \mathbf{exp(\Gamma t)Z(0)} + \mathbf{exp(\Gamma t)} \int_0^t \mathbf{exp(-\Gamma \tau)F(\tau)}\,\mathbf{d\tau}. \tag{28}$$

In general, the matrix $\mathbf{exp(\Gamma t)}$ is difficult to calculate. The modal analysis will be used in order to explicitly compute $\mathbf{Z(t)}$. First, the right and the left eigenvectors of the matrix $\mathbf{\Gamma}$ will be computed by

$$\begin{cases} \mathbf{\Gamma U}_i = \Omega_i \mathbf{U}_i, \\ \mathbf{\Gamma}^{\mathbf{t}} \mathbf{V}_i = \Omega_i \mathbf{V}_i, \end{cases} \tag{29}$$

where $\mathbf{\Gamma}'$ is the transpose of matrix $\mathbf{\Gamma}$, $\mathbf{U}_i$ is the right eigenvector and $\mathbf{V}_i$ is the adjoint eigenvector associated to the eigenfrequency Ω_i.

Let us assume that all eigenvalues are distinct, and then the eigenvectors $\mathbf{U}_i$ and $\mathbf{V}_i$ corresponding to different eigenvalues are biorthogonal. They can then be normalized and satisfy the following expressions:

$$\mathbf{V}_i^{\mathrm{T}} \mathbf{U}_j = \Omega_j \boldsymbol{\delta}_{ij}, \quad i,j = 1 \text{ to } 2(n+2). \tag{30}$$

Based on this transformation, the computation of the transition matrix is relatively easy. The system response is then given by

$$\begin{cases} \mathbf{Z(t)} = \mathbf{U[diag(exp(\Omega_i t))]V^{\mathrm{T}}Z_0} \\ \qquad + \mathbf{U[diag(exp(\Omega_i t))]} \int_0^t \mathbf{[diag(exp(-\Omega_i t))t]V^{\mathrm{T}}F(\tau)}\,\mathbf{d\tau}, \\ \mathbf{Z_0} = \begin{Bmatrix} \mathbf{W(0)} \\ \dot{\mathbf{W}}\mathbf{(0)} \end{Bmatrix}, \quad \mathbf{Z(t)} = \begin{Bmatrix} \mathbf{W(t)} \\ \dot{\mathbf{W}}\mathbf{(t)} \end{Bmatrix}. \end{cases} \tag{31}$$

Then, one can compute both the deflection $\mathbf{W(t)}$ and the velocity $\dot{\mathbf{W}}\mathbf{(t)}$ according to the initial conditions $\mathbf{W(0)}$, $\dot{\mathbf{W}}\mathbf{(0)}$ and to the external excitation $\mathbf{F(t)}$ at all internal points. For a specified point 'i', one gets:

$$W_i(t) = \sum_{m=1}^{2n+2} U_{im} \exp(\Omega_m t) \left\{ \sum_{j=1}^{2n+2} \left(V_{mj}^{\mathrm{T}} \dot{W}_j(0) + \int_0^t \exp(-\Omega_m \tau). \sum_{j=1}^{2n+2} V_{mj}^{\mathrm{T}} F_j(\tau)\,\mathrm{d}\tau \right) + \sum_{j=2n+1}^{2n+2} V_{mj}^{\mathrm{T}} W_j(0) \right\}. \tag{32}$$

For a simple explicit formulation, let us assume that $\mathbf{F(t)}$ is a unit impulse to the free end of the beam and $\mathbf{Z_0 = 0}$; i.e.: $\mathbf{F(t)} = \boldsymbol{\delta}\mathbf{(t)}\{\mathbf{0},\ldots,\mathbf{0},\mathbf{1}\}_{n+1}^{\mathbf{t}}$ where $\delta(t)$ is the Dirac delta function. In this case the deflection and velocity at all points are explicitly given by the simplified expressions:

$$\begin{cases} W_i(t) = \sum\limits_{m=1}^{2n+2} U_{im} \exp(\Omega_m t) \sum\limits_{j=1}^{2n+2} V_{mj}^{\mathrm{T}} F_j, \quad i = 1, n+2, \\ \dot{W}_i(t) = \sum\limits_{m=1}^{2n+2} U_{i+(n+2),m} \Omega_m \exp(\Omega_m t) \sum\limits_{j=1}^{2n+2} V_{mj}^{\mathrm{T}} F_j, \quad i = 1, n+2. \end{cases} \tag{33}$$

These explicit formulations allow one to investigate the dynamic response of damped beams subjected to various subtangential load parameters, stiffness and viscous parameters. For specified load and foundation

parameters, matrices in Eq. (24) have first to be computed following the developments presented in Appendix B. For numerical solutions, a computing program in MATLAB has been utilized. The MATLAB environment is exploited for a standard use of the presented formulation. The mathematical formulations presented are quite general and allow one to investigate the load–frequency dependence for beams on various types of elastic foundations, various subtangential parameter forces and various internal or viscous dampings. The frequencies and eigenmodes can be either real or complex. Therefore, at divergence instability the lowest frequency vanishes, as for conservative systems two frequencies can approach each other, coalesce and then become complex conjugates. Without damping, this corresponds to flutter instability and the load when the two frequencies coincide is defined as the flutter load. The load–frequency dependences and the flutter load corresponding to the coalescence of two natural frequencies are investigated. The mode, moment and shear force corresponding to the flutter load can be directly computed. The control of the flutter may also be performed based on internal or viscous damping. In the presence of damping, the flutter load is defined as the real part of the frequency becoming positive. Using Eqs. (29) and (33), the dynamic response is investigated at various load levels.

6. Numerical results and discussion

6.1. Flutter analysis

The flutter phenomena are investigated for a (C–F) beam loaded by a subtangential follower force (see Fig. 2). Without damping, the coalescence criterion is adopted. A uniform discretization is used with any number of internal points. The numerically obtained flutter load with 60 internal points is $\lambda^* = 20.0625$ ($\lambda^* = 20.05$ [29,31]) in case of $y = 1$ (Beck's problem). At this load, the first and the second eigenfrequencies coincide ($\omega_1^{*2} = \omega_2^{*2} = 121.46$) and become complex conjugates after the flutter load. The flutter load increases with respect to the subtangential angle 'y' and becomes $\lambda^* = 30.66$ for $y = 1.5$ ($\lambda^* = 30.63$ in Ref. [31]). Fig. 3 shows the load–frequency curves for a subtangential parameter $y = 1.5$ and the results are in perfect agreement with those presented in Ref. [31]. These tests permit validation of the results obtained by the presented methodological approach. Figs. 4 and 5 represent the load–frequency curves for various amplitudes and positions of the concentrated or uniform elastic foundations and the subtangential parameter '$y = 1.5$'. One can observe that action to the amplitude of the foundation causes a great change in the flutter value and particularly for $X_c = 1$. In order to highlight the transition from divergence to flutter and vice versa, more numerical results need to be investigated.

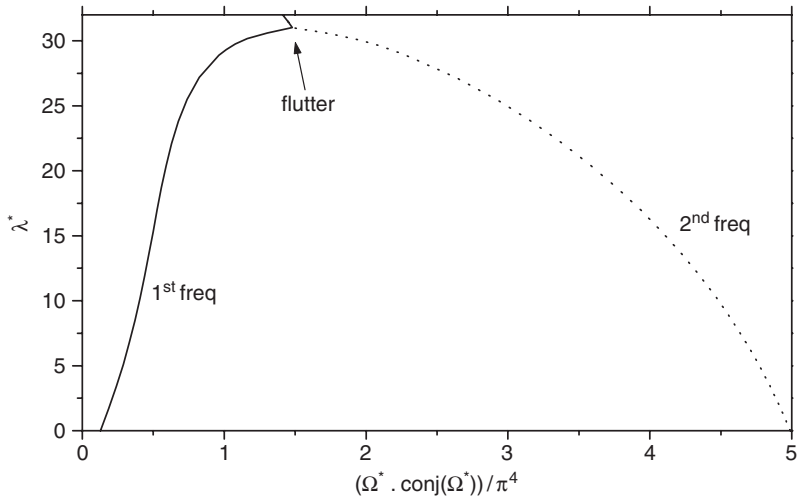

Fig. 3. Non-dimensional critical load λ^* versus non-dimensional frequency ω^* for a (C–F) beam. $y = 1.5$ and $\kappa^* = 0$. _____ : 1st frequency; …… : 2nd frequency.

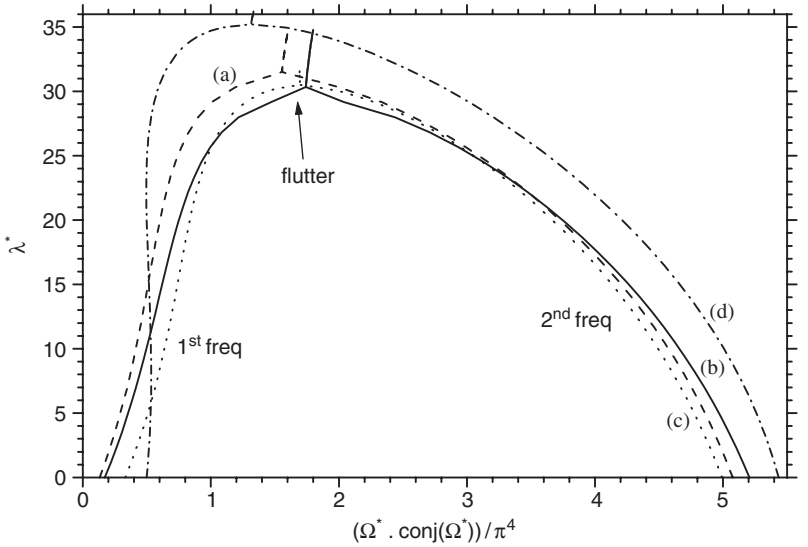

Fig. 4. Load–frequency curves for a (C–F) beam with $y = 1.5$ and $\kappa^* = 10$ at various concentrated points X_c: (a) $X_c = 0.25$; (b) $X_c = 0.5$; (c) $X_c = 0.75$; (d) $X_c = 1$.

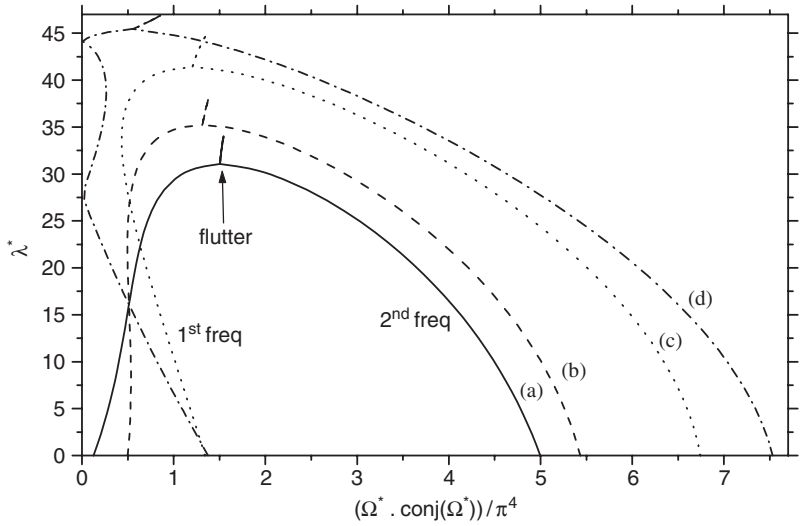

Fig. 5. Load–frequency curves for a (C–F) beam with $y = 1.5$ and various values of κ^*: (a) $\kappa_a^* = 0$; (b) $\kappa_a^* = 10$ at $X_c = 1$; (c) $\kappa_a^* = 30$ uniform; (d) $\kappa_a^* = 50$ at $X_c = 1$.

In Fig. 6, the evolution of the first, the second critical divergence and the critical flutter load according to the subtangential parameter 'y' and for different locations and values of the concentrated elastic foundation are presented. In Fig. 6a ($\kappa^* = 0$), one observes the jump phenomenon from $\lambda^* \approx 9.5$ to 16.04. This result is in good agreement with that obtained in Ref. [31] ($\lambda^* \approx 9.5$–16.5 graphically given in Ref. [31]). This jump is largely reduced for $\kappa^* = 10$ as shown in Fig. 6b.

Fig. 7 shows the critical load with respect to the concentrated elastic foundation position for various subtangential angles. Higher dependence between the flutter load, the position of the concentrated foundation and the subtangential parameter 'y' is demonstrated. For this test, additional information is supplied in order to explain its particular behavior. It is clearly shown that for $y = 0.3$ and $\kappa^* = 30$, the flutter position zone is largely reduced and there is no flutter for $X_c < 0.8$ or $X_c > 0.95$. For $y \geqslant 0.51$, the flutter may happen at every

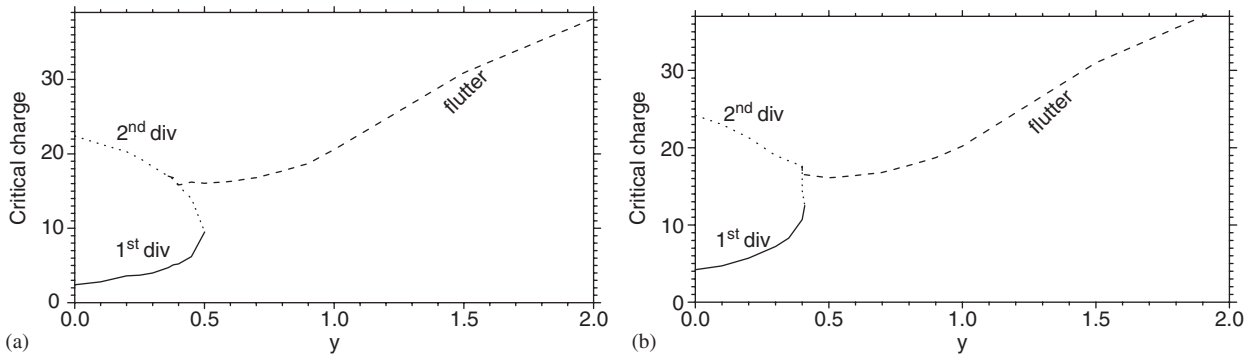

Fig. 6. Critical load according to the tangential angle coefficient 'y' of a cantilever beam for various amplitudes κ^* and positions X_c of the concentrated elastic foundation: (a) $\kappa_a^* = 0$; (b) $\kappa_a^* = 10$ at $X_c = 0.5$, _____: 1st divergence; …… : 2nd divergence; - - - - - : flutter.

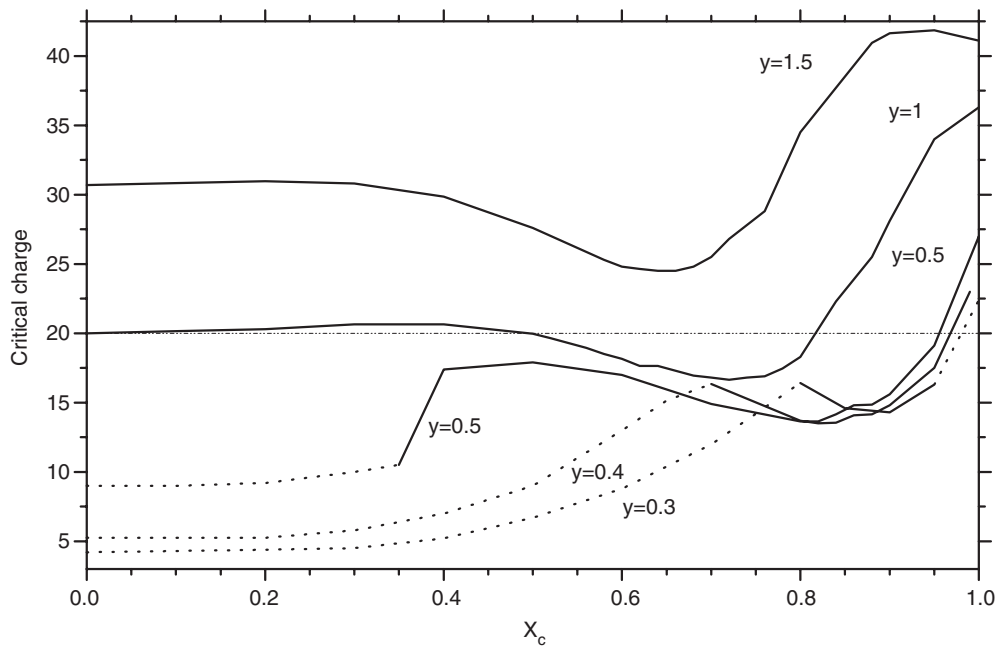

Fig. 7. Critical load for a (C–F) beam according to the position X_c of the concentrated elastic foundation ($k^* = 30$) for different y ($y = 0.365$ to $y = 1.5$). …… : divergence; _____: flutter.

position X_c. For '$y = 1$', the flutter load varies slowly from Beck's solution for $0 < X_c < 0.5$ and the variation increases greatly for $X_c \geqslant 0.8$. In the present analysis for $X_c = 1$ and $\kappa^* = 30$, the flutter limit corresponds to $y_{\lim} = 0.51$. For $y < y_{\lim}$, the flutter load is strongly position dependent and there is no flutter (divergence) for some positions. Fig. 7 also shows a general increasing trend of the critical flutter load when the position of the concentrated elastic foundation is located closer to the free end. However, if the location of the spring is near the clamped end, the variation of those values is very small. This means that if the designer decides to conceive a system with a beam subjected to a spring close to the free extremity, the assembly line associates must have a great preciseness to localize the spring.

The flutter and divergence zones with respect to κ^* and X_c are presented in Fig. 8. It can be noted that for '$y = 0.5$' and for each X_c there is a first limit value $\kappa^*_{\lim it,1}$ under which there is no flutter and the beam always diverges and a second limit value $\kappa^*_{\lim it,2}$ under which there is no divergence and the beam always flutters. At

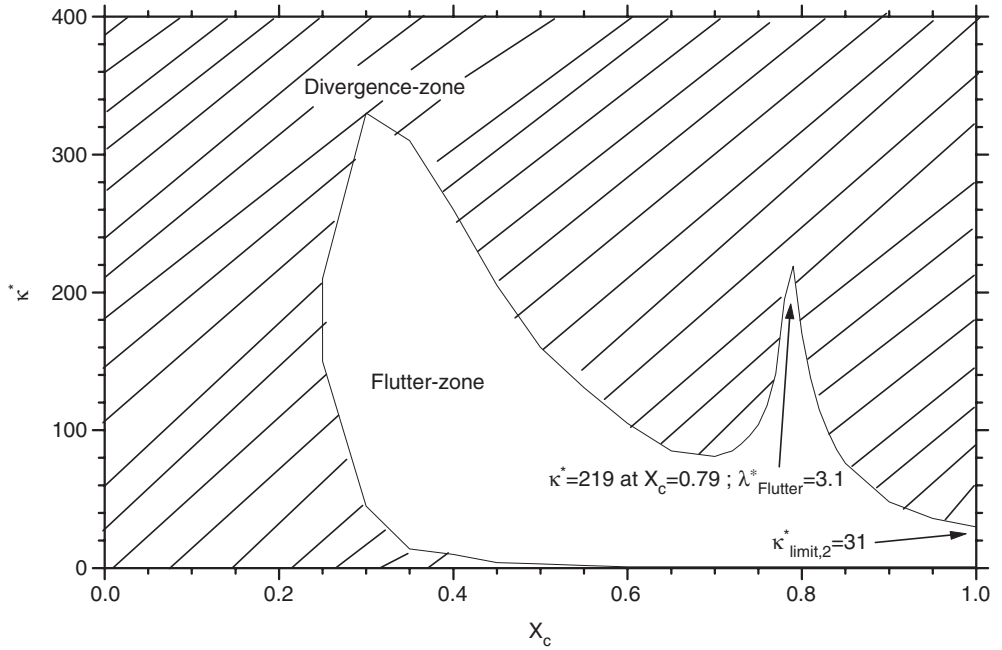

Fig. 8. Flutter limit and zone with respect to the amplitude and the position of concentrated foundation for a (C–F) beam. $y = 0.5$.

the beam end and for $y = 0.5$ (Fig. 8), those limit are $\kappa^*_{\lim it,1} = 1$ and $\kappa^*_{\lim it,2} = 31$. The flutter load is at its minimum for $\kappa^* \approx 219$ at $X_c = 0.79$ ($\lambda^*_{\text{flutter}} = 3.1$). This means that the beam will flutter for a very small value of load at this position. The change of the stability mechanism and the jump of the critical load with respect to various values of subtangential angle parameters and spring constant κ^* are illustrated in Fig. 9. For a cantilever beam on a concentrated elastic foundation at the free end ($X_c = 1$), when $y = 0.1$ and κ^* increases from 0, the critical load jumps first downwards and then upwards. At the same time, the type of instability mechanism first changes from divergence to flutter and then changes back to divergence. When $y = 0.3$ and κ^* increases from 0, the critical load jumps upwards twice. When $y = 1$, the critical load jumps downwards and the type of instability mechanism changes from flutter to divergence. This curve is consistent with the one given by Lee and Hsu [27]. However, in this paper, one can act on the position or even easier multiply the number of concentrated elastic foundations. These curves show clearly that the position of elastic foundation and the subtangential parameter have great effects on the dynamic stability phenomena.

For different values of a uniform κ^*, the load–frequency curves are represented in Fig. 10 for damped cantilevers with viscous damping and show clearly that the critical load is κ^*-independent. The same results and conclusion are reported in Ref. [24] using Galerkin's method.

The damping effect on the transition from flutter to divergence is also examined for various subtangential parameters 'y' and for different values of the concentrated elastic foundations κ^*. It is found that the flutter value decreases by a half in the presence of damping compared with the value without damping in the case of $\kappa^* = 0$. For the damping factor η^* varying between 0 and 0.005, the load–frequency curves are represented in Figs. 11a and b for $y = 1$ and $\kappa^* = 0$ ($\lambda_{\text{flutter}} \approx 11.2$) and in Figs. 12a and b for $y = 1$ and $\kappa^* = 30$ at $X_c = 1$ ($\lambda_{\text{flutter}} \approx 31.33$). The instability is of the flutter form. The smallest critical flutter load corresponds to the apex of the dome-shaped curves and there is no jump phenomenon. This can be also confirmed by examining the real part of the eigenvalue in Figs. 11b and 12b. Without damping, the real part of Ω^* is represented by the horizontal line on the upper position of the curve with the corresponding value of λ^*. With the presence of a slight amount of damping, the curves presented in Fig. 11b and 12b are found to commence in the negative ω^* region, intersect the λ^* axis and become positive at a flutter value which is much smaller than the undamped flutter load. With increased damping, the curves are found to diverge away from the λ^* axis and to approach an upper horizontal line (corresponding to the case without damping) asymptotically.

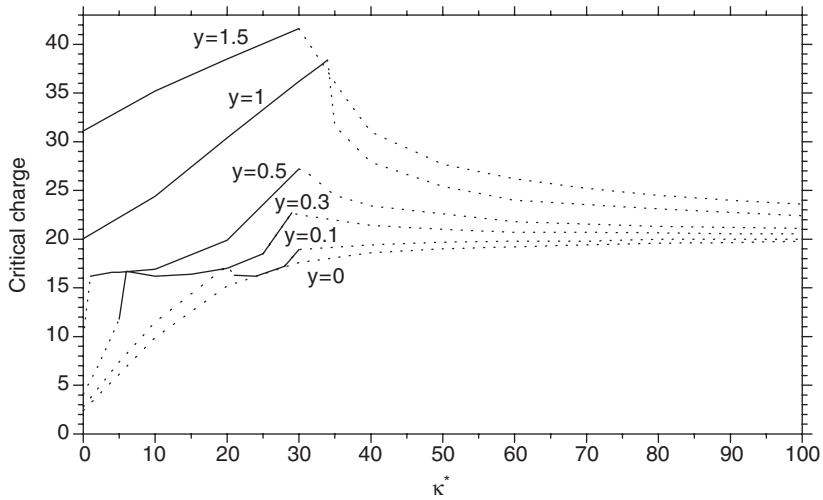

Fig. 9. Critical load versus the amplitude of elastic foundation concentrated at $X_c = 1$ for a (C–F) beam with various values of the tangential angle coefficient. …… : divergence; _____: flutter.

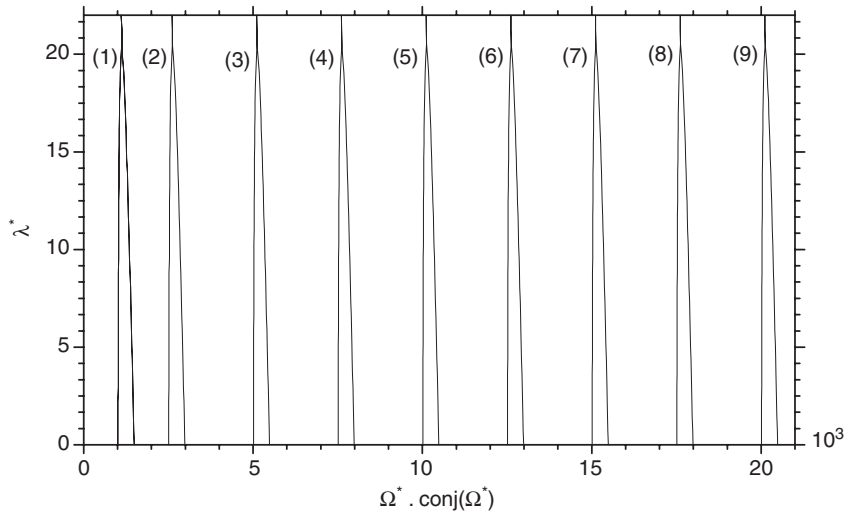

Fig. 10. Load–frequency curves of a cantilever rod subjected to a follower force on a uniform elastic foundation with κ^* varying between 1000 and 20 000 and viscous damping $\eta_v^* = 0.1$: (1) $\kappa^* = 1000$; (2) $\kappa^* = 2500$; (3) $\kappa^* = 5000$; (4) $\kappa^* = 7500$; (5) $\kappa^* = 10\,000$; (6) $\kappa^* = 12\,500$; (7) $\kappa^* = 15\,000$; (8) $\kappa^* = 17\,500$; (9) $\kappa^* = 20\,000$.

However, as is well known, the intersection point of these curves with the λ^* axis remains almost unaffected by the increase of the damping. It is clearly shown that the theoretical flutter load for undamped beam is reduced by a half for a damped beam even if the damping is very small. This means that damping cannot be neglected in flutter analysis. Furthermore, the flutter load is affected by small variations in the damping parameter. The damping effect in the instability of a beam with respect to parameters 'y' may at the same time produce a zone of instability by divergence and a zone of instability by flutter as presented in Figs. 13a and b (small divergence zone) and in Figs. 14a and b (large divergence zone). As the critical load is further increased, the real part of the eigenvalue shows a sharp turn towards the negative region of the diagram, making the loop structure observed in Figs. 13 and 14. The eigenvalue becomes positive again when the flutter occurs for λ^* very much larger than the critical divergence load. With the presence of a slight amount of damping, the real part of the

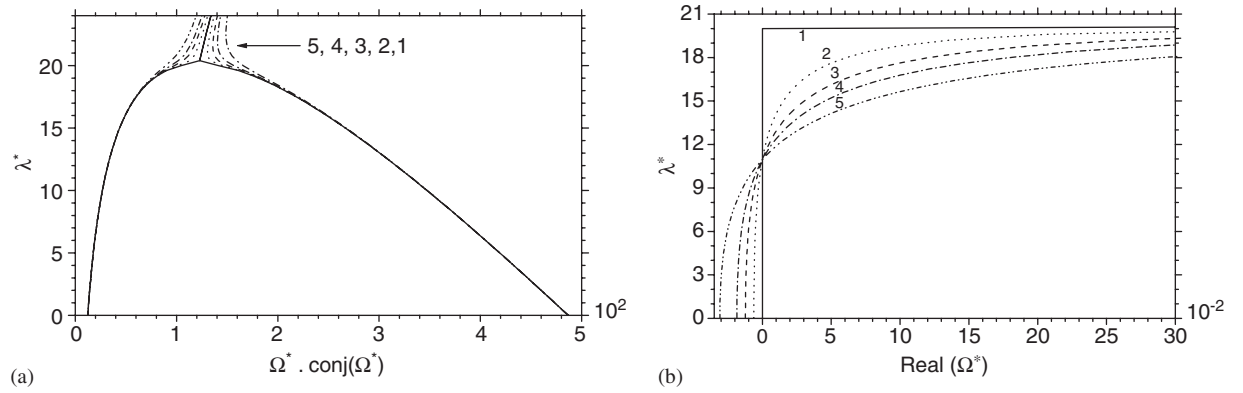

Fig. 11. Load–frequency curves of a damped cantilever beam subjected to a follower force ($y = 1$) and $\kappa^* = 0$: (1) $\eta^* = 0$; (2) $\eta^* = 0.001$; (3) $\eta^* = 0.002$; (4) $\eta^* = 0.003$; (5) $\eta^* = 0.005$.

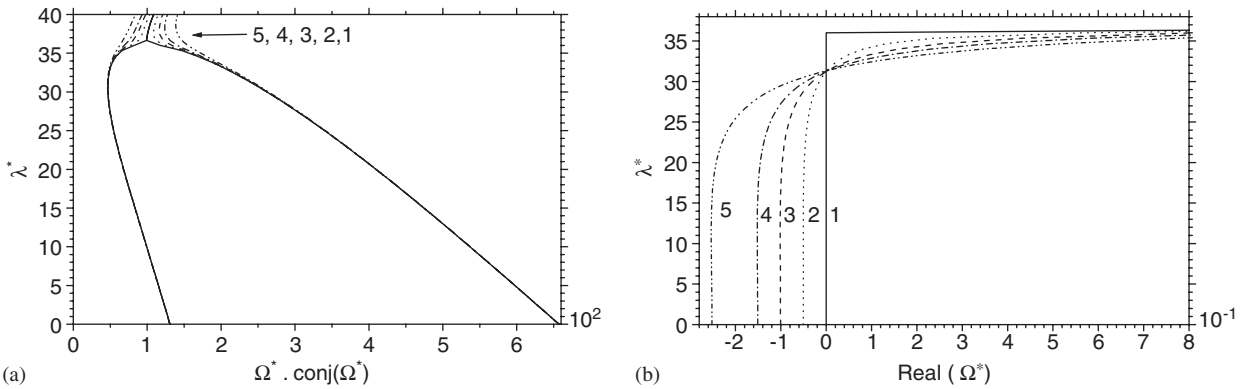

Fig. 12. Load–frequency curves of a damped cantilever beam subjected to a follower force ($y = 1$) and on an elastic foundation $\kappa^* = 30$ at $X_c = 1$: (1) $\eta^* = 0$; (2) $\eta^* = 0.001$; (3) $\eta^* = 0.002$; (4) $\eta^* = 0.003$; (5) $\eta^* = 0.005$.

eigenvalue remains positive for λ^* larger than the critical divergence load. However, the loop structure is relatively unaffected by the presence of damping. The remaining line patterns in Figs. 13 and 14 are caused by the presence of damping and are similar to the line patterns in Figs. 11 and 12 except for the presence of the loop structure. The critical divergence load is relatively unaffected by the presence of damping.

6.2. Dynamic response analysis

Consideration is now given to a (C–F) beam submitted to a subtangential follower axial force and to a unit transverse impulse at the free end. The dynamic response is given by the simplified formulation (33). In Fig. 15, dynamic responses and corresponding phase diagrams are represented for undamped and damped beams for various subtangential and damping parameters. One emphasizes particularly on situations such as: before flutter, at flutter and after flutter. The obtained results show a periodic motion for $\lambda^* = 0$, ($\Omega_1^2 = 12.3623$). As expected, for lateral conservative loads ($y = 0$), the dynamic response remains periodic (Fig. 15a) and the period of oscillations increases with λ^* and becomes infinite at buckling load [33]. The case of an undamped beam submitted to a non-conservative lateral load ($y = 1$) is represented in Fig. 15 and shows clearly that before the flutter, the dynamic response is periodic and the amplitude of oscillations remains constant (Fig. 15a). While after flutter this amplitude increases rapidly with time (Fig. 15c). For a lateral load close to the flutter load, the appearance of a 'beating' phenomenon is observed (Fig. 15b). The phase diagrams

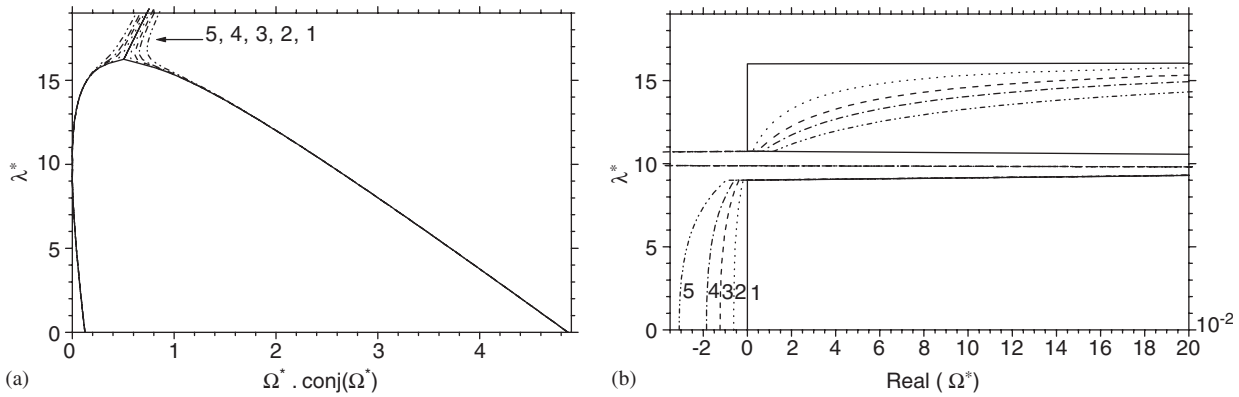

Fig. 13. Load–frequency curves of a damped cantilever beam subjected to a follower force ($y = 0.5$) and $\kappa^* = 0$: (1) $\eta^* = 0$; (2) $\eta^* = 0.001$; (3) $\eta^* = 0.002$; (4) $\eta^* = 0.003$; (5) $\eta^* = 0.005$.

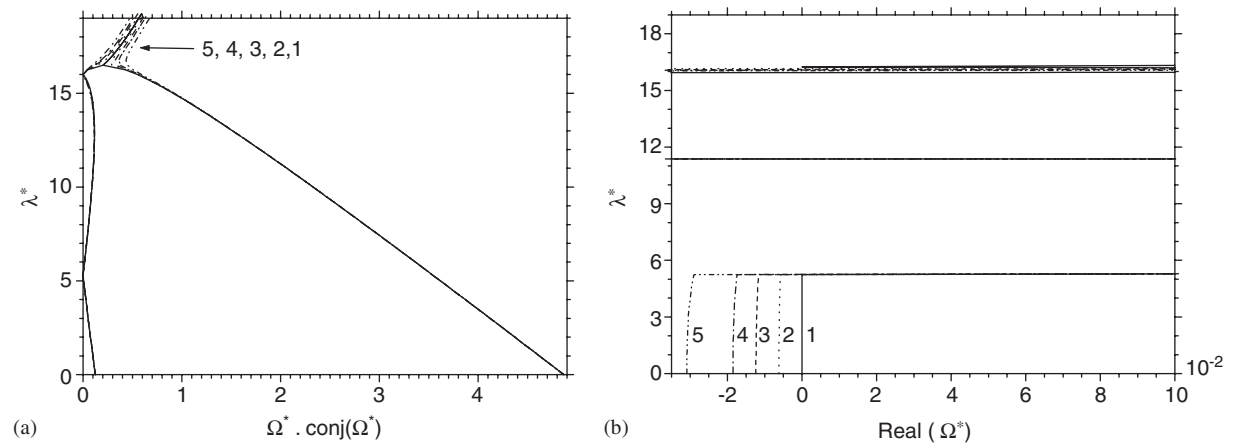

Fig. 14. Load–frequency curves of a damped cantilever beam subjected to a follower force ($y = 0.4$) and $\kappa^* = 0$: (1) $\eta^* = 0$; (2) $\eta^* = 0.001$; (3) $\eta^* = 0.002$; (4) $\eta^* = 0.003$; (5) $\eta^* = 0.005$.

are used to highlight these behaviors. For more general excitation forces, the dynamic response analysis can be obtained by formulation (31).

7. Conclusion

Integral equation formulation of the dynamic stability of a damped beam subjected to subtangential forces and on a viscoelastic foundation is presented. Based on a fundamental solution and radial basis functions, the governing partial differential equation is transformed into an algebro-differential system for the deflection, the slope, the moment and the shear force. Using a uniform discretization, a compact matrix formulation is presented for interior and boundary unknowns. The required matrices are explicitly given and the dynamic problem is formulated for unknowns at interior and boundary points. The flutter and divergence behaviors of beams are largely investigated based on an eigenvalue procedure. The amplitude and position of the viscoelastic foundation and subtangential parameter can be easily chosen in order to act on the flutter load. The present formulation is quite general and permits one to investigate the flutter loads, zones and the jump phenomenon in the follower force for the transition from flutter to divergence when the subtangential parameters (angle, load), the amplitude or position of a concentrated elastic foundation are slightly adjusted. The load–frequency diagrams due to variation of the above parameters are extensively presented in order to

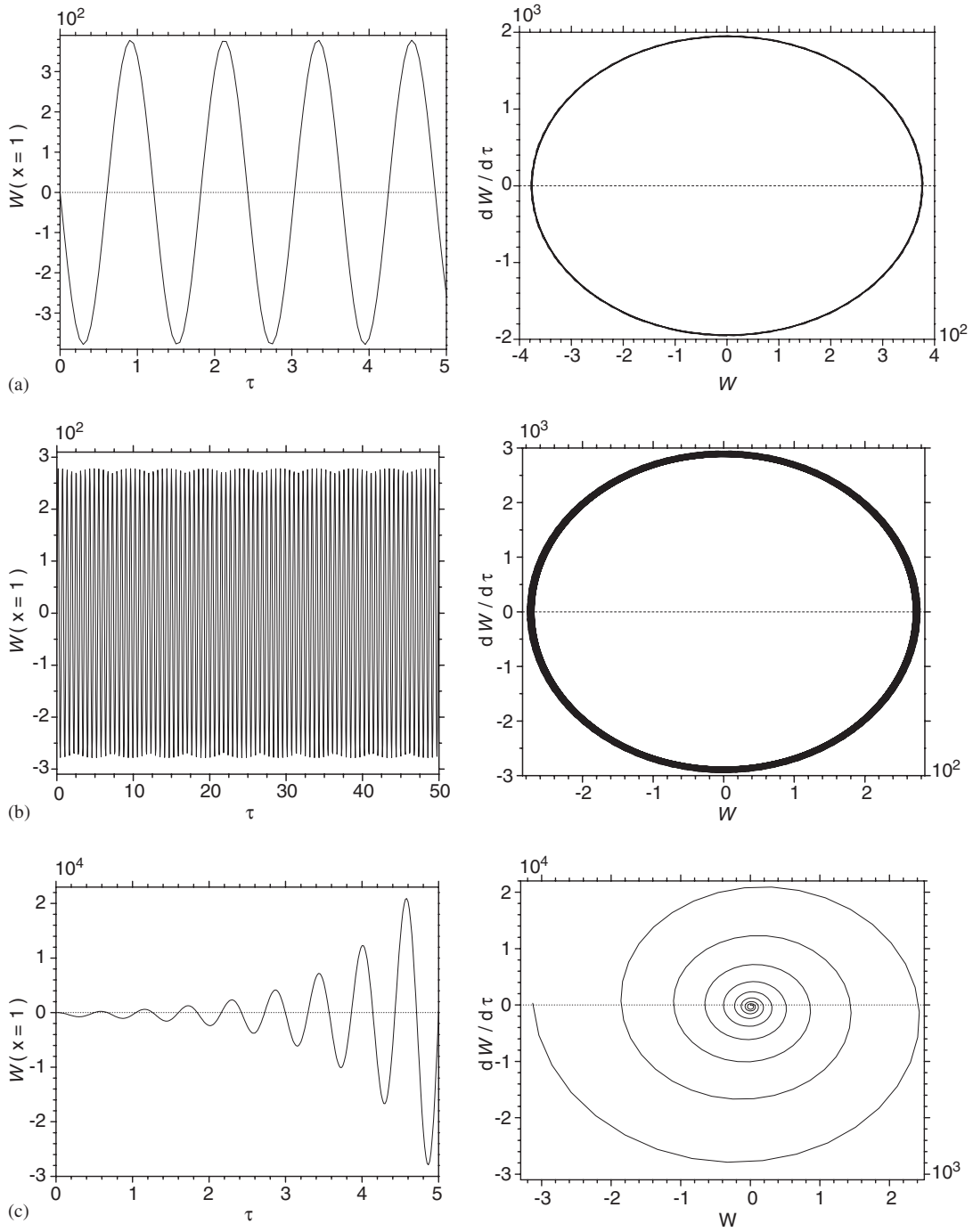

Fig. 15. Dynamic response and phase diagram of an undamped (C–F) beam at various follower load levels and $y = 1$ ($\lambda_{\text{flutter}} = 20.0625$): (a) before flutter $\lambda^* = 10$; (b) near flutter $\lambda^* = 20.1$; (c) after flutter $\lambda^* = 20.3$.

demonstrate the effectiveness of the presented methodological approach. Various types of damping are introduced in the formulation and their effects on the load–frequency dependence and dynamic response can be easily evaluated. Preliminary examination shows that for some cases, the modes of instability in the form of

flutter or divergence without damping, are found to be unaffected by the presence of slight damping although there may be a sharp decrease in the first critical load for instability by flutter. Based on the numerically computed eigenmodes, a compact formulation of the dynamic response and velocity are established. The dynamic response and phase diagrams of damped and undamped beams are presented at various subtangential load levels.

Acknowledgements

The authors wish to greatly thank the 'Ministère de l'Enseignement Supérieur et de la Recherche Scientifique' and the center 'CNRST' of Morocco and the center 'CNRS' of France for financial support from both projects: "PROTARS III (D11/22)" and "Action Intégrée (MA/05/117)".

Appendix A. Radial basis functions and fundamental solution used

In this study, we limit ourselves to isotropic elastic beams with a homogeneous and constant section. In this case, the rigidity and mass functions $K_1(x)$ and $K_2(x)$ are constant ($K_1(x) = K_2(x) = 1$).

The fundamental solution W^* used in this analysis corresponding to $(\partial^4 W^*/\partial x^4)(x,s) = \delta(x,s)$ is $W^*(x,s) = |x-s|^3/12$.

Several types of radial basis functions $f_j(x)$ are tested and the general form used is

$$f_j(x) = 1 + \alpha r_j + \beta r_j^2 + \gamma r_j^3 \quad \text{where } r_j = |x - x_j|.$$

The other functions g_j and h_j are calculated using the following expressions:

$$\frac{\mathrm{d}^4 g_j}{\mathrm{d}x^4}(x) = f_j(x) \quad \text{and} \quad \frac{\mathrm{d}^4 h_j}{\mathrm{d}x^4}(x) = k_2(x) f_j(x),$$

$$g_j(x) = h_j(x) = \frac{r_j^4}{24} + \alpha\frac{r_j^5}{120} + \beta\frac{r_j^6}{360} + \gamma\frac{r_j^7}{840},$$

where α, β and γ are chosen constants [4,6].

Appendix B. Matrices used

For the system of Eqs. (16) and (21), the used vectors and matrices have to be specified for the considered boundary condition. In this analysis, the beam is assumed to be clamped–free as presented in Fig. 2. This corresponds to

$$W_1 = 0, \quad \theta_1 = 0, \quad M_{N+2} = 0 \quad \text{and} \quad Q_{n+2} = -\kappa^*(w_{n+2} + \upsilon^* \dot{w}_{n+2}) + (1-y)\lambda^* \theta_{n+2}.$$

The matrices used in the analyses are as follows ($s_i = (i-1)/(n+1)$):

G1: matrix $((n+2) \times (n+2))$ of radials functions,

$$\begin{cases} G1_{ij} = f_j(s_i), \quad i = 1, n+2; \quad j = 1, n+2, \\ \text{the other terms are null.} \end{cases}$$

G: matrix $((n+2) \times (n+2))$,

$$\begin{cases} G_{ij} = G1^{-1}_{i(j+1)} \quad i = 1, n+2; \quad j = 1; n+1. \\ \text{Because for C}-\text{F boundary conditions } W_1 = 0, \text{ the other terms are null.} \end{cases}$$

O: matrix $(2 \times (n+2))$,

$$\begin{cases} O_{1,n+1} = -\dfrac{\kappa^*}{4}, \\ O_{1,n+2} = -0.5, \\ O_{2,n+2} = 0.5, \\ \text{the other terms are null.} \end{cases}$$

A: matrix $((n+2) \times 2)$,

$$\begin{cases} A_{i1} = -\dfrac{s_{i+1}^2}{4}, \quad i = 1; n+1, \\ A_{i2} = \dfrac{s_{i+1}^3}{12}, \quad i = 1; n+1, \\ A_{n+2,1} = A_{n+2,2} = 0. \end{cases}$$

$\mathbf{A}'$: matrix (2×2),

$$\begin{cases} A'_{11} = A'_{12} = 0, \\ A'_{21} = -\frac{1}{2}, \quad A'_{21} = \frac{1}{4}. \end{cases}$$

I: matrix $((n+2) \times (n+2))$,

$$\begin{cases} I_{i,i} = 1, \quad i = 1; n, \\ I_{i,n+1} = \kappa^* \dfrac{(1 - s_{i+1})^3}{12} - \dfrac{1}{2}, \quad i = 1; n, \\ I_{n+1,n+1} = 0.5, \\ I_{n+2,n+1} = \dfrac{\kappa^*}{12} - \dfrac{1}{2}, \\ I_{i,n+2} = \dfrac{(1 - s_{i+1})}{2}, \quad i = 1; n+1, \\ I_{n+2,n+2} = 0.5, \\ \text{the other terms are null.} \end{cases}$$

B: $\mathbf{B} = \mathbf{B1G}$, **B1** matrix $((n+2) \times (n+2))$,

$$\begin{cases} B1_{ij} = B_j(s_{i+1}), \quad i = 1, n+1; \quad j = 1, n+2, \\ B1_{n+2,j} = B_j(0), \quad j = 1, n+2. \end{cases}$$

$\mathbf{B}'$: $\mathbf{B}' = \mathbf{B1}'\mathbf{G}$, $\mathbf{B1}'$ matrix $(2 \times (n+2))$,

$$\begin{cases} B1'_{1j} = \hat{B}_j(0), \quad j = 1, n+2, \\ B1'_{2j} = \hat{B}_j(1), \quad j = 1, n+2. \end{cases}$$

H: matrix $((n+2) \times (n+2))$,

$$\begin{cases} H_{i,n+1} = \dfrac{(1 - s_{i+1})^3}{12}, \quad i = 1, n+1 \\ H_{n+2,n+1} = \frac{1}{12}, \\ \text{the other terms are null.} \end{cases}$$

$\mathbf{H}'$: matrix $(2 \times (n+2))$,

$$\begin{cases} H'_{1,n+1} = -\frac{1}{4}, \\ \text{the other terms are null.} \end{cases}$$

C: $\mathbf{C} = \mathbf{C1G}$, **C**1 matrix $((n+2)\times(n+2))$,

$$\begin{cases} C1_{ij} = C_j(s_{i+1}), & i = 1, n+1; \quad j = 1, n+2, \\ C1_{n+2,j} = C_j(0), & j = 1, n+2. \end{cases}$$

C′: $\mathbf{C}' = \mathbf{C1}'\mathbf{G}$, **C1**′ matrix $(2\times(n+2))$,

$$\begin{cases} C1'_{1j} = \hat{C}_j(0), & j = 1, n+2, \\ C1'_{2j} = \hat{C}_j(1), & j = 1, n+2. \end{cases}$$

J: matrix $((n+2)\times(n+2))$,

$$\begin{cases} J_{i,n+2} = \dfrac{(1-s_{i+1})^3}{12}, & i = 1, n+1, \\ J_{n+2,n+2} = \frac{1}{12}, \\ \text{the other terms are null.} \end{cases}$$

J′: matrix $(2\times(n+2))$,

$$\begin{cases} J'_{1,n+2} = -\frac{1}{4}, \\ \text{the other terms are null.} \end{cases}$$

For a concentrated elastic foundation at x_c:
D: matrix $((n+2)\times(n+2))$,

$$\begin{cases} D_{i,x_c} = W^*(x_c, s_{i+1}) = \dfrac{|x_c - s_{i+1}|^3}{12}, & i = 1, n+1, \\ D_{n+2,x_c} = W^*(x_c, 0) = \dfrac{x_c^3}{12}, \\ \text{the other terms are null.} \end{cases}$$

D′: matrix $(2\times(n+2))$,

$$\begin{cases} D'_{1,x_c} = \hat{W}^*(x_c, 0) = -\dfrac{x_c^2}{4}, \\ D'_{2,x_c} = \hat{W}^*(x_c, 1) = -\dfrac{|x_c - 1|^2}{4}, \\ \text{the other terms are null.} \end{cases}$$

P: vector $(1\times(n+2))$,

$$\begin{cases} P_i = P(s_{i+1}), & i = 1, n+1, \\ P_{n+2} = P(0). \end{cases}$$

P′: vector (1×2),

$$\begin{cases} P'_1 = \hat{P}(0), \\ P'_2 = \hat{P}(1). \end{cases}$$

References

[1] V.V. Bolotin, *Non Conservative Problems of the Theory of Elastic Stability*, Pergamon Press, New York, 1963.
[2] H. Ziegler, *Principle of Structural Stability*, Blaisdell Publishing Compan, Toronto, 1968.
[3] H. Leipholz, *Stability of Elastic Systems*, Sijthoff & Noordhoff, The Netherlands, 1980.
[4] V.V. Bolotin, Dynamic instabilities in mechanics of structures, *Applied Mechanical Review* 52 (1999) R1–R9.

[5] M.A. Langthjem, Y. Sugiyama, Dynamic stability of columns subjected to follower loads: a survey, *Journal of Sound and Vibration* 238 (5) (2000) 809–851.
[6] D. Nardini, C.A. Brebbia, in: C.A. Brebbia (Ed.), *A New Approach to Free Vibration Analysis using Boundary Elements Boundary Element Method in Engineering*, Springer, Berlin, 1982, pp. 313–326.
[7] D.E. Beskos, Boundary element methods in dynamic analysis. Part II (1986–1996), *Applied Mechanical Review ASME* 50 (1997) 149–197.
[8] P.W. Partridge, C.A. Brebbia, L.W. Wrobel, *The Dual Reciprocity Boundary Element Method*, Computational Mechanics Publications, Southampton, 1992.
[9] J.R. Chang, W. Yeih, J.T. Chen, Determination of the natural frequencies and natural mode of a rod using the dual BEM in conjunction with the domain partition technique, *Computational Mechanic* 24 (1999) 29–40.
[10] M. Tanaka, W. Chen, Dual reciprocity BEM applied to transient elstodynamic problems with differential quadrature method in time, *Computer Methods in Applied Mechanics and Engineering* 190 (2001) 1347–2331.
[11] G. Rong, H. Kisu, C. Huang, A new algorithm for bending problems of continuous and inhomogeneous beam by the BEM, *Advances in Engineering Software* 30 (5) (1999) 339–346.
[12] M. Schanz, H. Antes, A Boundary integral formulation for the dynamic behavior of a Timoshenko beam, Advances in Boundary Element Techniques, Vol. II, Hoggar, 2001, pp. 475–482.
[13] E.J. Sapountzakis, Solution of non uniform torsion of bars by an integral equation method, *Computers and Structures* 77 (2000) 659–667.
[14] J.T. Katsikadelis, G.C. Tsiatas, Non linear dynamic analysis of beams with variable stiffness, *Journal of Sound and Vibration* 270 (2004) 847–863.
[15] M. Levinson, Application of the Galerkin and Ritz method to non conservative problems of elastic stability, *ZAMP* 17 (1966) 431–442.
[16] M.A. De Rosa, C. Franciosi, The influence of an intermediate support on the stability behavior of cantilever beams subjected to follower forces, *Journal of Sound and Vibration* 137 (1990) 107–115.
[17] L.M. Zorii, Y.A. Chermokha, Influence of support condition on dynamic stability of elastic column, *Prikladnaya Mekhanika* 7 (1971) 134–136.
[18] A.N. Kounadis, On static stability analysis of elastically restrained structures under follower forces, *AIAA* 18 (1980) 176–473.
[19] N. Kounadis, Divergence and flutter instability of elastically restrained structures under follower forces, *International Journal of Engineering Science* 19 (1981) 553–562.
[20] N. Kounadis, The existence of regions of divergence instability for unconservative systems under followers force, *International Journal of Solids and Structures* 19 (1983) 725–733.
[21] I. Elishakoff, J. Hollkamp, Computerized symbol solution for a non conservative system in which instability occurs by flutter in one range of a parameter and by divergence in another, *Computer Methods in Applied Mechanics and Engineering* 62 (1987) 27–46.
[22] H.P. Lee, Dynamic instability of a rod with an intermediate spring support subjected to a substantial follower forces, *Computer Methods in Applied Mechanics and Engineering* 125 (1995) 141–150.
[23] H.P. Lee, Divergence and flutter of a cantilever rod with an intermediate spring support, *International Journal of Solids and Structures* 32 (10) (1995) 1371–1382.
[24] H.P. Lee, Flutter and divergence instability of non conservative beams and plates, *International Journal of Solids and Structures* 33 (10) (1995) 1409–1424.
[25] H.P. Lee, Damping effects on the dynamic stability of a rod subjected to intermediate follower loads, *Computer Methods in Applied Mechanics and Engineering* 131 (1–2) (1996) 147–157.
[26] H.P. Lee, Flutter of a cantilever rod with a relocatable lumped mass, *Computer Methods in Applied Mechanics and Engineering* 144 (1–2) (1997) 23–31.
[27] S.Y. Lee, K.C. Hsu, Elastic instability of beams subjected to a partially tangential force, *Journal of Sound and Vibration* 186 (1) (1995) 111–123.
[28] Q. Wang, S.T. Quek, Enhancing flutter and buckling capacity of column by piezoelectric layers, *International Journal of Solids and Structures* 39 (16) (2002) 4167–4180.
[29] A.M. Gasparini, A.V. Saetta, R.V. Vitaliani, On the stability and instability regions of non-conservative continuous system under partially follower forces, *Computer Methods in Applied Mechanics and Engineering* 124 (1–2) (1995) 63–78.
[30] Si-Ung Ryu, Y. Sugiyama, Computational dynamics approach to the effect of damping on stability of a cantilevered column subjected to a follower force, *Computers and Structures* 81 (4) (2003) 265–271.
[31] Q.H. Zuo, H.L. Schreyer, Flutter and divergence instability of non conservative beams and plates, *International Journal of Solids and Structures* 33 (9) (1996) 1355–1367.
[32] Z. El Felsoufi, L. Azrar, Modélisation des vibrations des poutres à section variable par la méthode des équations intégrales, *Proceedings du 6éme congrès de mécanique*, Vol. 1, Tanger, Maroc, avril, 2003, pp. 7–8.
[33] Z. El Felsoufi, L. Azrar, Buckling, flutter and vibration analyses of beams by integral equation formulations, *Computers and Structures* 83 (2005) 2632–2649.